

# I $\kappa$ B Kinase $\beta$ Promotes Cell Survival by Antagonizing p53 Functions through $\Delta$ Np73 $\alpha$ Phosphorylation and Stabilization<sup>∇</sup>

Rosita Accardi,<sup>1</sup> Mariafrancesca Scalise,<sup>1</sup> Tarik Gheit,<sup>1</sup> Ishraq Hussain,<sup>1</sup>† Jiping Yue,<sup>1</sup>  
Christine Carreira,<sup>1</sup> Agnese Collino,<sup>1</sup>‡ Cesare Indiveri,<sup>2</sup> Lutz Gissmann,<sup>3</sup>  
Bakary S. Sylla,<sup>1\*</sup> and Massimo Tommasino<sup>1\*</sup>

International Agency for Research on Cancer, 150 Cours Albert-Thomas, 69008 Lyon, France<sup>1</sup>; Università della Calabria, Via Ponte Pietro Bucci, Cubi 4C-6C, 87036 Arcavacata di Rende (CS), Cosenza, Italy<sup>2</sup>; and Deutsches Krebsforschungszentrum, Im Neuenheimer Feld 280, 69120 Heidelberg, Germany<sup>3</sup>

Received 18 August 2010/Returned for modification 21 September 2010/Accepted 27 March 2011

**$\Delta$ Np73 $\alpha$ , a dominant-negative inhibitor of p53 and p73, exhibits antiapoptotic and transforming activity in *in vitro* models and is often found to be upregulated in human cancers. The mechanisms involved in the regulation of  $\Delta$ Np73 $\alpha$  protein levels in normal and cancer cells are poorly characterized. Here, we show that that I $\kappa$ B kinase beta (IKK $\beta$ ) increases  $\Delta$ Np73 $\alpha$  protein stability independently of its ability to activate NF- $\kappa$ B. IKK $\beta$  associates with and phosphorylates  $\Delta$ Np73 $\alpha$  at serine 422 (S422), leading to its accumulation in the nucleus, where it binds and represses several p53-regulated genes. S422A mutation in  $\Delta$ Np73 $\alpha$  abolished IKK $\beta$ -mediated stabilization and inhibition of p53-regulated gene expression. Inhibition of IKK $\beta$  activity by chemical inhibitors, overexpression of dominant-negative mutants, or gene silencing by siRNA also resulted in  $\Delta$ Np73 $\alpha$  destabilization, which under these conditions was rapidly translocated into the cytoplasm and degraded by a calpain-mediated mechanism. We also present evidence for the IKK $\beta$  and  $\Delta$ Np73 $\alpha$  cross talk in cancer-derived cell lines and primary cancers. Our data unveil a new mechanism involved in the regulation of the p73 and p53 network.**

p53 and its family members, p63 and p73, are transcription factors that play an important role in the regulation of the cell cycle, apoptosis, and cancer development (4, 23). All three proteins show similarity in the amino acid sequences of their N-terminal transcription activation (TA), DNA binding, and oligomerization domains. p73 and p53 are also functionally related, since they have the ability to bind a similar set of p53 regulatory elements (REs) (16). Both proteins are functionally regulated by posttranslational modifications, and p73 appears to be subject to more complex regulatory mechanisms than p53 at transcriptional level. The p73 gene is expressed as multiple isoforms that differ in their N and/or C terminus. The generation of different transcripts of p73 involves the use of two distinct promoters (P1 and P2) and/or alternative splicing. The mRNA of the full-length p73 isoform (TAp73) is transcribed by the P1 promoter located upstream of exon 1, while an isoform called  $\Delta$ Np73 is generated by using the P2 promoter in intron 3 (P2). Three additional  $\Delta$  isoforms,  $\Delta$ N'p73,  $\Delta$ Ex2p73, and  $\Delta$ Ex2/3p73, arise from alternative splicing of the transcripts originating from the first exons. All  $\Delta$ N isoforms lack the TA domain located at the N terminus (exons 2 and 3). Multiple splicing of exons 10 to 14 generate additional TA and

$\Delta$ N p73 isoforms ( $\alpha$ ,  $\beta$ ,  $\gamma$ ,  $\delta$ ,  $\epsilon$ ,  $\zeta$ ,  $\theta$ ,  $\eta$ , and  $\eta$ 1) that differ at the C terminus, affecting the biological properties of p73 isoforms (19, 30). For instance,  $\Delta$ Np73 $\beta$  induces cell cycle arrest and apoptosis, while  $\Delta$ Np73 $\alpha$  exerts antiapoptotic functions and promotes cellular transformation (21).

The antiapoptotic function of  $\Delta$ Np73 $\alpha$  can be explained by at least two mechanisms. In the first,  $\Delta$ Np73 $\alpha$  competes with p53 for binding to p53 REs and prevents the activation of p53- or p73-regulated genes. In the second,  $\Delta$ Np73 $\alpha$  associates with TAp73 to form transcriptionally inactive heterodimer complexes (4, 23). Thus,  $\Delta$ Np73 $\alpha$  acts as a dominant-negative inhibitor of p53 and p73 transcriptional functions.

High  $\Delta$ Np73 levels have been found in a number of human malignancies, including cancers of the breast, prostate, liver, lung, and thyroid (4). Overexpression of  $\Delta$ Np73 $\alpha$  in cancer cell lines inhibits the expression of p53/p73-regulated genes and increases proliferation (13, 15, 34). In addition, high levels of  $\Delta$ Np73 $\alpha$  in cancer cells with wild-type p53 and/or p73 functions correlate with increased drug resistance (4, 23). Accordingly, an unfavorable prognosis of some cancers is correlated with high  $\Delta$ Np73 expression levels (8, 22).

Several mechanisms that influence TAp73 protein levels have been elucidated. Similar to the case with p53, p73 half-life and activity are regulated by posttranslational modifications, such as phosphorylation and acetylation (2, 7, 11, 12, 14, 27, 33). Upon induction of DNA damage by cisplatin, p73 is phosphorylated at three distinct sites by Chk1, c-Abl, and PKC $\delta$  (2, 11, 12, 27, 33). In addition, a more recent study showed that the same DNA damaging agent induces the translocation of I kappa B kinase  $\alpha$  (IKK $\alpha$ ) in the nucleus, which in turn phosphorylates TAp73 at the N terminus, increasing its stability

\* Corresponding author. Mailing address: Infections and Cancer Biology Group, International Agency for Research on Cancer, 150 Cours Albert-Thomas, 69008 Lyon, France. Phone: 33 4 72 73 81 91. Fax: 33 4 72 73 84 42. E-mail for Bakary S. Sylla: sylla@iarc.fr. E-mail for Massimo Tommasino: tommasino@iarc.fr.

† Present address: Division of Biochemistry, SK University of Agricultural Sciences & Technology of Kashmir, Shuhama, Alusteng, Kashmir, India.

‡ Present address: Istituto Europeo di Oncologia, Milan, Italy.

<sup>∇</sup> Published ahead of print on 11 April 2011.

TABLE 1. Sequences of different siRNAs used for gene silencing

Target	siRNA sequence or description (source)
IKK $\alpha$ gene	5'-GCAGGCUCUUUCAGGGACA-3'
IKK $\beta$ gene	5'-CGUACGCGGAAUACUUCGA-3'
p65 gene	siGenome SMART pool M-003533-02-0005, human RELA, NM_021975 (Thermo Scientific)
Scrambled (negative control)	5'-GGUGGAAGAGUGGUGAGC-3'

(10). In contrast to p73, very little is known about the events involved in controlling  $\Delta$ Np73 levels.

Here we describe a novel mechanism that regulates the protein levels and activity of  $\Delta$ Np73 $\alpha$  via phosphorylation by IKK $\beta$ , which leads to stabilization of  $\Delta$ Np73 $\alpha$  and stimulation of its prosurvival activity.

MATERIALS AND METHODS

**Expression vectors.** Cellular and viral genes were expressed using the retroviral vector pBabe (24) or pLXSN (Clontech, Palo Alto, CA) and the expression vector pcDNA-3 (Invitrogen). The pLXSN-HPV38 E6/E7 construct has been previously described (5). The following constructs were generated during this study, using standard molecular biology techniques: pBabe-puro-FlagDN-IKK, pBabe-puro  $\Delta$ N-Ik $\beta$  lacking the first N-terminal 36 amino acids (kindly provided by Thomas Gilmore, Boston University), pcDNA3 HA- $\Delta$ Np73 $\alpha$  mutants (A159 A163, A418 A422, A418, A422, and A521 A525 mutants), and pcDNA3 HA- $\Delta$ Np73 $\alpha$  deletion mutants (amino acids 1 to 300, 1 to 450, or 350 to 587). pcDNA-Flag-Ik $\beta$  wild type was provided by Thomas Gilmore (Boston University). pcDNA3 wild-type HA- $\Delta$ Np73 $\alpha$  and - $\beta$  were kindly provided by Takashi Tanaka (Columbia University, New York), while pRK5-Flag-IKK $\alpha$ , pRK5-Flag-IKK $\beta$ , and pRK5-Myc-tagged IKK $\beta$  deletion mutants (amino acids 1 to 303 or 304 to 756) were kindly provided by David Goeddel (Tulirak, San Francisco, CA).

**Cell culture procedures.** Keratinocyte cultures and generation of high-titer retroviral supernatants were carried out as previously described (5). Saos-2, HNC-136, human embryonic kidney (HEK293), HCC1937, and Cal-51 cells and mouse embryonic fibroblasts (MEFs) were cultured in fetal calf serum (FCS) and Dulbecco's modified Eagle medium (DMEM) (Gibco) using standard culturing conditions. Wild-type and IKK null MEFs were kindly provided by Inder Verma (Salk Institute, San Diego, CA). Cells were transiently transfected with the different expression vectors by using FuGENE6 reagent (Roche).

Gene silencing of IKK $\alpha$  and - $\beta$  was obtained using synthetic small interfering RNA (siRNA) (Table 1). siRNA or scrambled RNA at a concentration of 50 nM was transfected using Oligofectamine according to the standard protocol (Invitrogen).

Downregulation of  $\Delta$ Np73 $\alpha$  was achieved by transfecting the antisense (AS) oligonucleotide as previously described (1).

**Pulse-chase labeling.** For metabolic labeling, 24 h after transfection, HEK293 cells were grown for 1 h at 37°C in DMEM lacking L-methionine (Gibco) and pulsed for 1 h with 50  $\mu$ Ci/ml of EasyTag L-[<sup>35</sup>S]methionine (Perkin Elmer). Afterwards, cells were washed with phosphate-buffered saline and chased with complete culture medium for 4, 8, and 12 h. Then, cells were washed in cold phosphate-buffered saline and collected. Cellular pellets were stored at -80°C until further analysis.

**In vitro cell treatments.** Cells were treated with the Ik $\beta$  kinase inhibitor Bay11-7082 (20  $\mu$ M) (Calbiochem) for 2 h. The proteasome inhibitors MG132 (CBZ-Leu-Leu-Leu-al) (50  $\mu$ M) (Sigma) and lactacystin (10  $\mu$ M) (Calbiochem), calpain inhibitor PD150606 (50  $\mu$ M) (Calbiochem), calpain inhibitor VI (150  $\mu$ M) (Calbiochem), and cysteine protease inhibitor E-64 (30  $\mu$ M) (Calbiochem) were added to the culture medium for 8 h. Tumor necrosis factor alpha (TNF- $\alpha$ ) (B&D) was used at the final concentration of 10 ng/ml at different time points, as indicated in each specific experiment. For the determination of  $\Delta$ Np73 $\alpha$  half-life cells were treated with cycloheximide as previously described (1). An *in vitro* calpain cleavage assay was performed as previously described (25).

For *in vitro* protein dephosphorylation, samples were treated with 100 U of  $\lambda$  phosphatase (BioLabs) for 30 min at 30°C.

For ionizing radiation treatment, cells were trypsinized and resuspended in DMEM containing 10% FCS. Afterwards, cells were irradiated with a dose of 30 Gy.

TABLE 2. Sequences of primers used for RT-PCR analyses, for ChIP, and for cloning<sup>a</sup>

Promoter or gene for:	Primer sequence
Mouse $\Delta$ Np73	F: 5'-GTGACCCCATGAGACACCTC-3' R: 5'-GTATGTCCAGGTGGCCGAC-3'
Mouse GAPDH	F: 5'-GCCAAAAGGGTCATCATC-3' R: 5'-TGCCAGTGAGCTTCCCGTTC-3'
$\Delta$ Np73	F: 5'-AACCATGCTGTACGTCGGGTGACCC-3' R: 5'-GCGACATGGTGTGCAAGGTGG-3'
GAPDH	F: 5'-AAGGTGGTGAAGCAGGCGT-3' R: 5'-GAGGATGGGTGTGCTGTGT-3'
Pig3	F: 5'-GCTTCAAATGGCAGAAAAGC-3' R: 5'-AACCCATCGACCATCAAGAG-3'
Pig3 <sup>b</sup>	F: 5'-CCCAGGACTGCGTTTTGCCT-3' R: 5'-GTCCATTTCCAGGCATGG-3'
p21 <sup>b</sup>	F: 5'-CGAGGCAGGCCAAGGG-3' R: 5'-GCAGAGGATGGATTGTTCA-3'
HA- $\Delta$ Np73 (1-300)	F: 5'-AAAAAAGCTTATGTATCCATACGATGTCCTGATTACGCTATGCTGTACGTCGGTGACC-3'
HA- $\Delta$ Np73 (1-450)	F: 5'-AAAAAAGCTTATGTATCCATACGATGTCCTGATTACGCTATGCTGTACGTCGGTGACC-3'
HA- $\Delta$ Np73 (300-587)	F: 5'-AAAAAAGCTTATGTATCCATACGATGTCCTGATTACGCTATGGAGACGAGGACACGTA-3'
	R: 5'-AAAAGCGGCCGCTCAGTGGATCTCGCTCCCGT-3'

<sup>a</sup> F, forward; R, reverse.  
<sup>b</sup> Promoter.

**RT-PCR.** Total cellular RNA was extracted from cells or tissues using the Absolutely RNA Miniprep kit (Stratagene). Reverse transcriptase (RT)-PCR analyses were carried out as described previously (5). The primer sequences used for RT-PCR are indicated in Table 2.

**Immunoblotting and antibodies.** Total protein extracts, sodium dodecyl sulfate (SDS)-polyacrylamide gel electrophoresis (PAGE), and immunoblotting were prepared as described by Accardi et al. (1). The following antibodies were used:  $\beta$ -actin (C4; MP Biomedicals), human p53 (NCL-CM1; Novocastra Laboratories Ltd.), p73 (anti-p73 Ab-1; Calbiochem), IKK $\beta$  and IKK $\alpha$  (Upstate), hemagglutinin (HA)-peroxidase-high affinity (3F10; Roche), Flag antibody (M5; Sigma), c-Myc (Sigma), mouse p73 (Ab-2; NeoMarkers), phospho-Ik $\beta$  Ser32/36 (9246), Ik $\beta$  (9242), and p21<sup>WAF1/CIP1</sup> (DCS60 2946) from Cell Signaling, and anti-IgG (Diagenode).

The anti-phosphoserine 422  $\Delta$ Np73 antibody was generated by Biogenes. A synthetic peptide, C-Nle-SSSH-pS-AQS-Nle-V-amide, conjugated with the carrier protein lactase-phlorizin hydrolase, was synthesized. Six boosts were administered to the rabbits over a period of 3 months. Final bleedings were collected, and monospecific IgG was purified over affinity columns.

**Immunoprecipitation.** For immunoprecipitations of overexpressed proteins, total cell extracts (250  $\mu$ g) were precleared with Sepharose CL-6B for 1 h at 4°C. After preclearing, total protein extracts were mixed with 40  $\mu$ l Flag M2-conjugated beads (Sigma), 50  $\mu$ l of anti-c-Myc agarose-conjugate (Sigma), or 1  $\mu$ g of anti-HA antibody mixed with 30  $\mu$ l of protein A/G Sepharose (Roche) and incubated overnight at 4°C. Beads were extensively washed in lysis buffer and analyzed by immunoblotting. Anti-IKK $\beta$  antibody (Upstate) and anti- $\Delta$ Np73 (IMG-313A; Imgenex) were used to immunoprecipitate endogenous IKK $\beta$  and  $\Delta$ Np73 using 1 to 2 mg of total extracts of 38E6E7HFK, HNC-136, HCC1937, and Cal-51 cells.

Chromatin immunoprecipitation (ChIP) was performed with Diagenode Shearing ChIP and OneDay ChIP kits according to the manufacturers' protocols.

**Immunofluorescence.** Immunofluorescence staining of monolayer cultured keratinocytes was performed on cells grown on cover slides and fixed with 4% formaldehyde, permeabilized with PBS-0.1% Triton X, and stained using the following primary antibodies: anti-human  $\Delta$ Np73 (IMG-313A; Imgenex), anti-rabbit IKK $\beta$  (Millipore), and anti-p65 (Santa Cruz). Alexa Fluor 488 goat anti-rabbit IgG(H+L) and Alexa Fluor 532 goat anti-mouse IgG(H+L) were used as

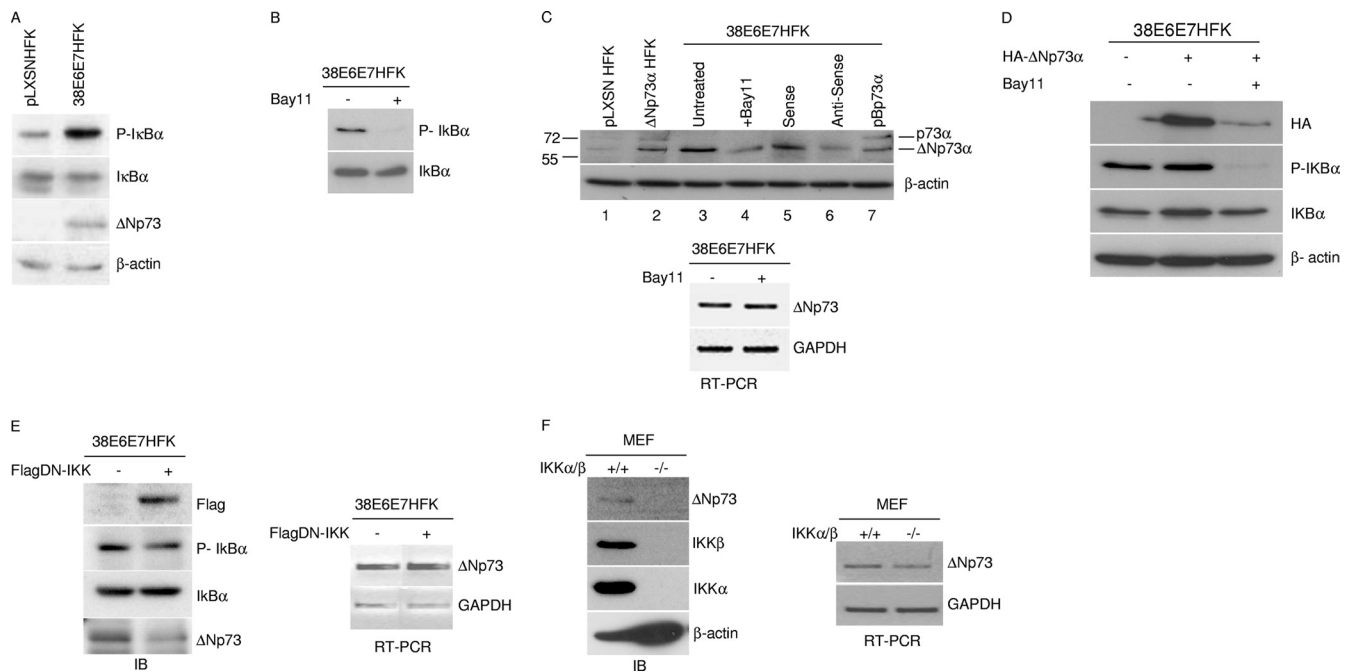


FIG. 1. The IKK complex regulates the stability of the  $\Delta$ Np73 protein. (A) Protein extracts of primary keratinocytes transduced with empty retrovirus vector (pLXSN HFK) or immortalized keratinocytes expressing HPV type 38 E6 and E7 (38E6E7HFK) were analyzed by immunoblotting with the indicated antibodies. (B) 38E6E7HFK cells were treated with Bay11 or dimethyl sulfoxide (DMSO) for 2 h. Protein extracts were prepared and analyzed by immunoblotting with the indicated antibodies. (C) Protein extracts of pLXSN HFKs or HFKs stably expressing  $\Delta$ Np73 $\alpha$  or p73 $\alpha$ , 38E6E7HFK cells, or 38E6E7HFK cells cultured in the presence of Bay11 or transfected with  $\Delta$ Np73 sense or antisense oligonucleotide were analyzed by immunoblotting with the indicated antibodies (upper panel). Total RNA was also extracted from Bay11-treated 38E6E7HFK cells, and  $\Delta$ Np73 or GAPDH mRNA levels were measured by RT-PCR (bottom panel). (D) 38E6E7HFK cells were transfected with a HA- $\Delta$ Np73 $\alpha$  construct. Cells were treated with Bay11 or DMSO for 2 h and processed as for panel A. (E) 38E6E7HFK cells were transduced with a pBabe-puro (pBp) or pBp-flagged dominant-negative kinase-dead IKK (Flag-DN-IKK) retrovirus. Protein extracts were analyzed by immunoblotting with the indicated antibodies (left panel). Total RNA was also extracted from both cell lines, and  $\Delta$ Np73 or GAPDH mRNA levels were measured by RT-PCR (right panel). (F) Protein extracts from wild-type MEFs (IKK $\alpha$ / $\beta$ <sup>+/+</sup>) and IKK $\alpha$ / $\beta$ <sup>-/-</sup> MEFs were prepared and analyzed by immunoblotting using the indicated antibodies (left panel). Total RNA was prepared from wild-type or IKK $\alpha$ / $\beta$  knockout MEFs, and the levels of  $\Delta$ Np73 transcript were determined by RT-PCR (right panel).

secondary antibodies. The slides were mounted using mounting medium containing DAPI (4',6-diamidino-2-phenylindole) (H-1200; Vectashield) and analyzed with an immunofluorescence Axioplan2 microscope from Zeiss or by confocal laser scan microscopy (Leica). For fluorescence resonance energy transfer (FRET), cells were fixed, permeabilized, and stained as explained above. As secondary antibodies, the combination of Alexa 488 (donor) and Alexa 555 (acceptor) was used. After staining, cells were analyzed using the Leica TCS SP5 II spectral confocal system. To measure FRET, three images were acquired sequentially in the same order through the following: (i) an Alexa 488 filter set (excitation, 488 nm; emission, 520 to 580 nm; filter at 488 nm), (ii) an Alexa 555 filter set (excitation, 543 nm; emission, 590 to 700 nm; filter at 540 nm), and (iii) a FRET filter set (excitation, 488 nm; emission, 580 to 700 nm; filter at 540 nm) according to methods in previous publications (6, 26).

**Immunohistochemistry.** Normal ( $n = 2$ ) and invasive breast cancers ( $n = 1$  grade I specimen;  $n = 1$  grade II specimen; and  $n = 3$  grade III specimens) were provided and histologically examined by L. Frappart (Pathology Department, Hospital E. Herriot, Lyon, France). Processing of the specimens was performed in accordance with the ethical guidelines for handling of human material. Immunohistochemical stainings were carried out on 3- $\mu$ m sections and performed on serial sections, using the antibody anti-human  $\Delta$ Np73 (1:500; Imgenex), anti-mouse IKK $\beta$  (1:300; Upstate), or  $\Delta$ Np73 $\alpha$ -P-422S antibody. Preincubation of  $\Delta$ Np73 $\alpha$ -P-422S antibody with phosphorylated or unphosphorylated  $\Delta$ Np73 $\alpha$  peptide was performed at room temperature for 30 min. Immunohistochemical signal was revealed with the Vectastain EliteABC kit (PK 6102; Vector Laboratories) according to the manufacturer's protocol. Images (magnification,  $\times 40$ ) were taken with a Nikon Eclipse E600 camera. The intensity of nuclear staining was quantified by the color deconvolution

technique with the Common Centre of Quantimetry (CCQ) (UBCL, Lyon, France).

**In vitro kinase assay.** *In vitro* phosphorylation of  $\Delta$ Np73 by IKK $\beta$  was performed by combining 2  $\mu$ g of the glutathione *S*-transferase (GST) fusion proteins with the IKK $\beta$  immunoprecipitated from HPV38 expressing keratinocytes pretreated or not with Bay11. The reaction was performed in 30  $\mu$ l of kinase buffer (20 mM HEPES, 10 mM MgCl<sub>2</sub>, 1 mM dithiothreitol [DTT], 10 mM *p*-nitrophenyl phosphate (PNPP), 100 mM  $\beta$ -glycerol-3-phosphate, 25  $\mu$ M NaV, and 40  $\mu$ M cold ATP) and 20  $\mu$ Ci of [ $\gamma$ -<sup>32</sup>P]ATP (Perkin Elmer) at 30°C for 30 min. The reaction was terminated by the addition of SDS-PAGE sample buffer. Lysates were separated by SDS-PAGE (12%), transferred to nitrocellulose, and visualized on X-ray films.

**In vivo <sup>32</sup>P protein labeling.** HEK293 cells were transfected with the different constructs as appropriate. After 24 h, cells were grown for 3 h in serum-free and phosphate-free medium and then incubated with 0.3 mCi/ml of [<sup>32</sup>P]orthophosphate for three additional hours. Cells were lysed in lysis buffer (20 mM Tris-HCl [pH 8], 200 mM NaCl, 0.5% Nonidet P-40, 1 mM EDTA, 10 mM KCl, 1 mM DTT, 50 mM NaF, 50 mM  $\beta$ -glycerophosphate, 1 mM Na orthovanadate, and 0.1  $\mu$ M okadaic acid) and immunoprecipitated with 1  $\mu$ g of anti-HA-tag antibody (Roche). The immunoprecipitates were separated on a 10% SDS gel. The gel was dried and exposed to an X-ray film. The same experiment was performed in parallel in the absence of [<sup>32</sup>P]orthophosphate and analyzed by immunoblotting. The amount of radioactivity incorporated on the HA- $\Delta$ Np73 protein was measured by using a PhosphorImager (445-SI) and quantified by the ImageQuant software program (Molecular Dynamics). The protein levels were quantified as described by Accardi et al. (1).

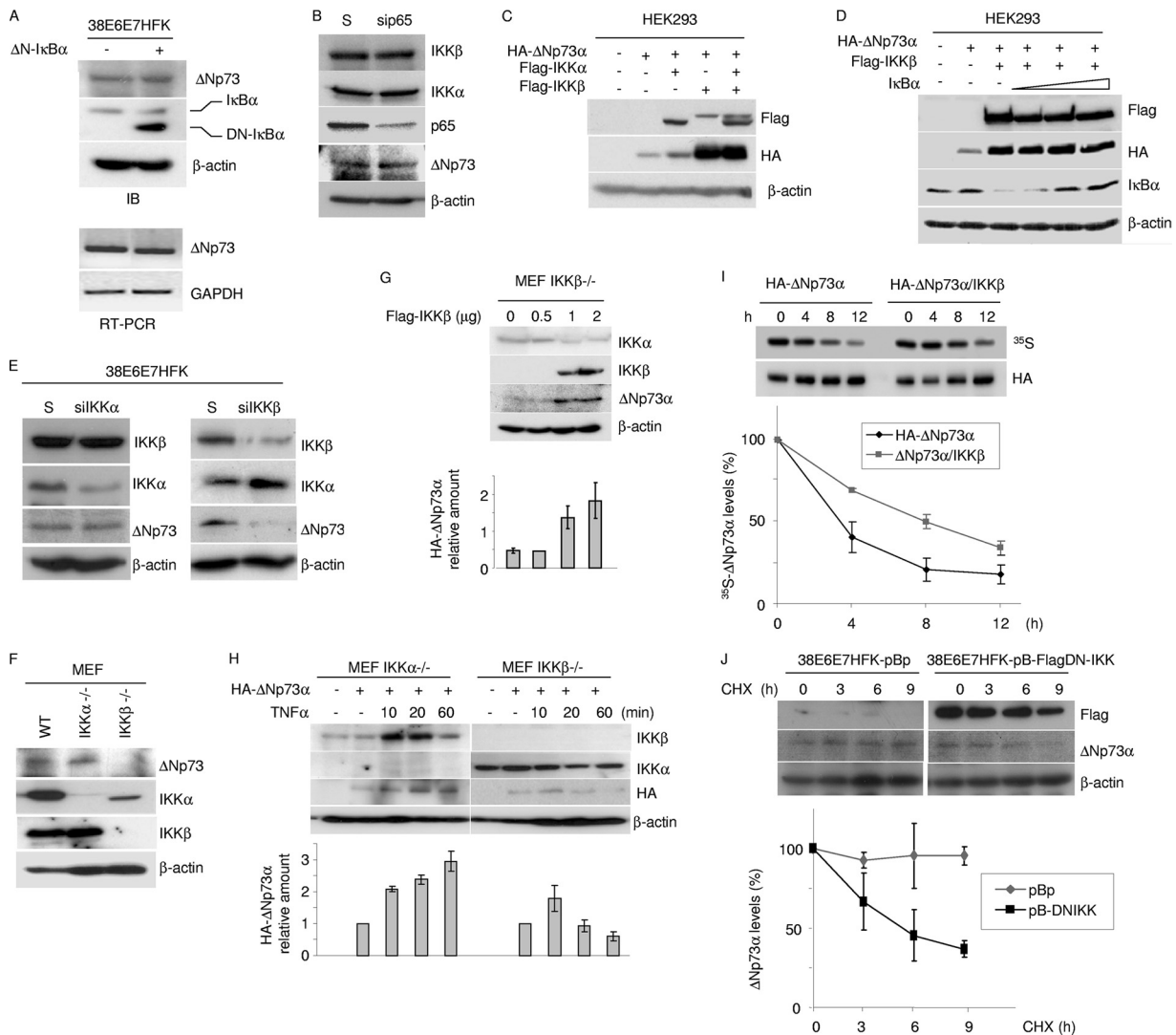


FIG. 2. IKK $\beta$  increases  $\Delta$ Np73 protein levels. (A) 38E6E7HFK cells were transfected with pBp or with pBp- $\Delta$ N- $\text{I}\kappa\text{B}\alpha$  superrepressor ( $\Delta$ N- $\text{I}\kappa\text{B}\alpha$ ). Protein extracts were analyzed by immunoblotting using the indicated antibodies (top panel). Total RNA was also extracted from both cell lines, and  $\Delta$ Np73 or GAPDH mRNA levels were measured by RT-PCR (bottom panel). (B) Scrambled (S) RNA and siRNA for p65 (sip65) was transfected in 38E6E7HFK cells. Thirty-six hours after transfection, protein extracts were analyzed by immunoblotting with the indicated antibodies. (C and D) HEK293 cells were transfected with different expression constructs as indicated. After 24 h, protein extracts were analyzed by immunoblotting with the indicated antibodies. (E) Scrambled (S) RNA and siRNA for IKK $\alpha$  (siIKK $\alpha$ ) or IKK $\beta$  (siIKK $\beta$ ) was transfected in 38E6E7HFK cells. Thirty-six hours after transfection, protein extracts were analyzed by immunoblotting with the indicated antibodies. (F) IKK $\alpha$ / $\beta$ <sup>+/+</sup> (WT), IKK $\alpha$ <sup>-/-</sup>, and IKK $\beta$ <sup>-/-</sup> MEF cellular protein extracts were analyzed by immunoblotting with the indicated antibodies. (G) IKK $\beta$ <sup>-/-</sup> MEF cells were transfected with increasing concentrations of pcDNA3-Flag-IKK $\beta$ , and 24 h after transfection, protein extracts were analyzed by immunoblotting with the indicated antibodies (top panel). The  $\Delta$ Np73 protein signal was quantified by the Quantity One software program (Bio-Rad), normalized on the levels of  $\beta$ -actin, and the values obtained were reported in the histogram (bottom panel). The data are the means of results from two independent experiments. (H) IKK $\alpha$ <sup>-/-</sup> MEF and IKK $\beta$ <sup>-/-</sup> MEF cells were transfected with pcDNA3-HA- $\Delta$ Np73 $\alpha$  and treated with TNF- $\alpha$  at the indicated time points. Protein extracts were analyzed by immunoblotting with the indicated antibodies (top panel). The amounts of HA- $\Delta$ Np73 signal in the Western blot were quantified as explained for panel G and are reported in the histogram (bottom panel). The data are the means of results from two independent experiments. (I) HEK293 cells were transfected with HA-tagged  $\Delta$ Np73 $\alpha$  in the absence or presence of overexpressed Flag-tagged IKK $\beta$ . Twenty-four hours after transfection, cells were labeled for 1 h with L- [<sup>35</sup>S]methionine, chased for the indicated times, and collected. Following anti-HA immunoprecipitation, the immunocomplexes were loaded on an SDS-PAGE gel and transferred onto a polyvinylidene difluoride (PVDF) membrane. Autoradiography (top panel) and then anti-HA Western blotting (middle panel) were performed; <sup>35</sup>S-HA- $\Delta$ Np73 bands were quantified by Image Lab (Bio-Rad) and normalized on the total levels of immunoprecipitated HA- $\Delta$ Np73 protein. The percentage of  $\Delta$ Np73 at time zero was referred to as 100%, and the percentages of protein at the different time points were calculated relative to that at time zero and reported in the histogram (lower panel). The data are the means of results for two independent experiments. (J) 38E6E7HFK cells stably expressing a dominant-negative inhibitor of IKK $\beta$  (pB-FlagDN-IKK) were generated and cultured in the presence of CHX for the indicated number of hours. At each time point, cells were collected. Protein extracts were prepared and analyzed by immunoblotting with the indicated antibodies (upper panel). The levels of  $\Delta$ Np73 were quantified by Quantity One (Bio-Rad) and normalized on the levels of  $\beta$ -actin. The percentages of  $\Delta$ Np73 at the different time points were calculated as for Fig. 1G and are reported in the histogram (lower panel). The data are the means of results for two independent experiments.

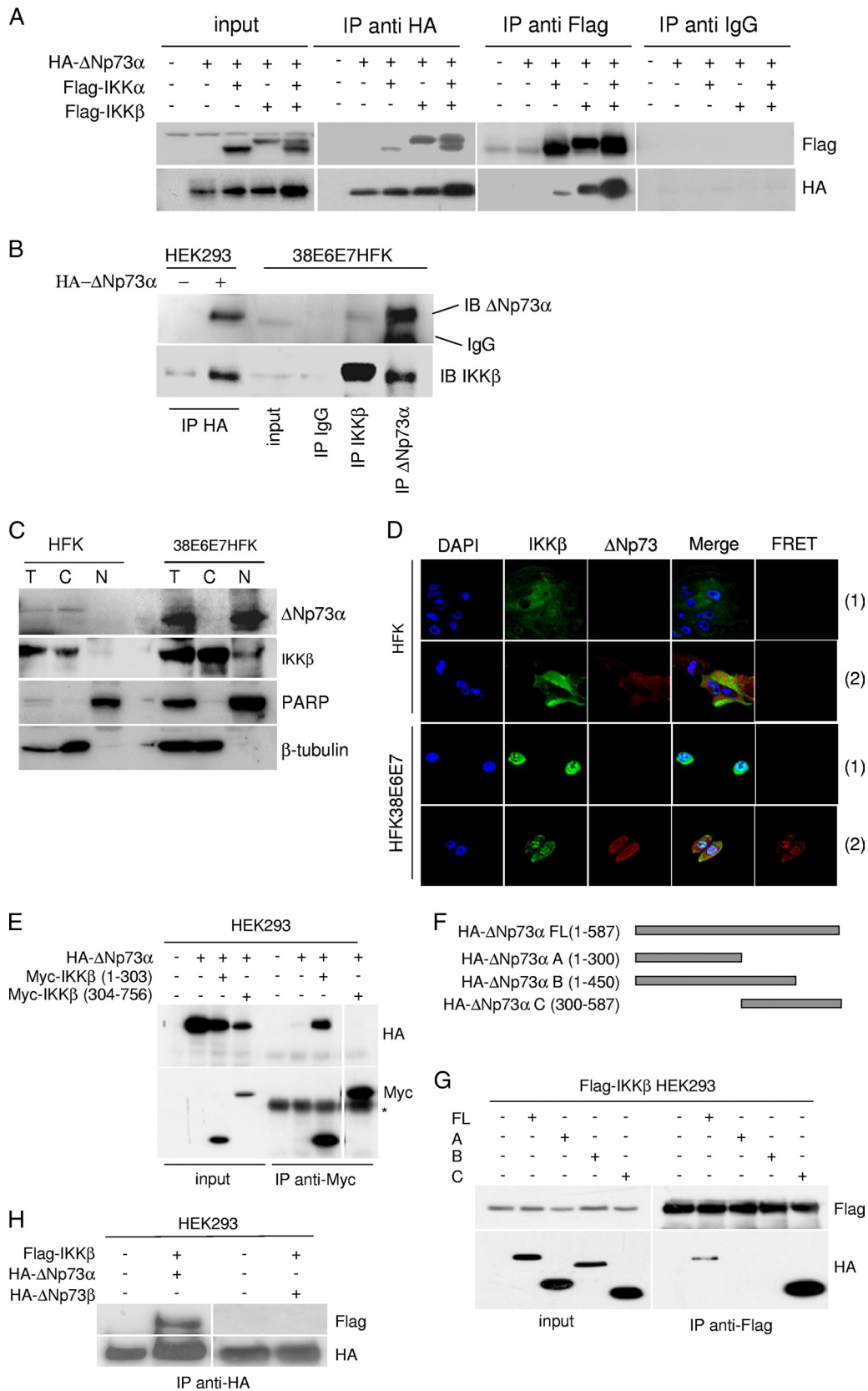


FIG. 3. IKKβ directly interacts with ΔNp73. (A) HEK293 cells were transfected with the indicated expression plasmids, and 24 h after transfection, protein extracts were subjected to immunoprecipitation followed by immunoblotting. “Input” represents 1/10 of total extracts used for the immunoprecipitation. (B) One-milligram protein extracts of 38E6E7HFK cells were immunoprecipitated with the indicated antibodies,

## RESULTS

**IKK pathway influences  $\Delta$ Np73 $\alpha$  protein levels.** Based on previous findings on the ability of IKK $\alpha$  to stabilize TAp73 (10), we evaluated whether  $\Delta$ Np73 $\alpha$  stability could be regulated by the NF- $\kappa$ B pathway. We used human foreskin keratinocytes expressing the E6 and E7 oncoproteins of human papillomavirus (HPV) type 38 (38E6E7HFK) that, as previously shown, express high  $\Delta$ Np73 $\alpha$  levels and not other p73 isoforms (1). As shown in Fig. 1A, I $\kappa$ B $\alpha$  was found to be hyperphosphorylated in 38E6E7HFK cells in comparison to primary keratinocytes (pLXSNHFK). The phosphorylation and degradation of I $\kappa$ B $\alpha$  is mediated by activated IKK $\alpha$  and IKK $\beta$  in the canonical pathway of NF- $\kappa$ B; thus, our findings indicate that IKK complex is constitutively activated in these cells. Inhibition of IKK by the chemical compound Bay11-7082 (Bay11) led to a reduction in I $\kappa$ B $\alpha$  phosphorylation (Fig. 1B) and in the levels of 60- to 65-kDa protein, which is recognized by an anti-p73 antibody and most likely corresponds to  $\Delta$ Np73 $\alpha$  (Fig. 1C, top panel, compare lanes 3 and 4). Indeed, this protein comigrated with the ectopically expressed  $\Delta$ Np73 $\alpha$  in HFKs (Fig. 1C, lane 2). In addition, its expression was significantly decreased by antisense oligonucleotides specific for the  $\Delta$ Np73 isoforms and showed a migration different from that of p73 (Fig. 1C, top panel, lanes 5 to 7). In contrast to protein levels, Bay11 treatment did not significantly alter  $\Delta$ Np73 $\alpha$  transcript levels (Fig. 1C, bottom panel). Similar results were obtained when a hemagglutinin (HA) tag- $\Delta$ Np73 $\alpha$  fusion protein (HA- $\Delta$ Np73 $\alpha$ ) was ectopically expressed in 38E6E7HFK cells. In fact, immunoblotting using HA tag antibody showed that  $\Delta$ Np73 $\alpha$  protein levels were strongly affected by Bay11 treatment (Fig. 1D). Similar to Bay11 treatment, blocking IKK signaling pathways by overexpressing a dominant-negative mutant of IKK $\beta$  (DN-IKK) in 38E6E7HFK cells also resulted in reduced levels of phospho-I $\kappa$ B $\alpha$  and a decrease in  $\Delta$ Np73 $\alpha$  protein levels (Fig. 1E, left panel), while no significant changes in  $\Delta$ Np73 $\alpha$  mRNA levels were observed (Fig. 1E, right panel). Finally, immunoblotting with an antibody that recognizes exclusively the  $\Delta$ Np73 form in mouse embryo fibroblasts (MEFs) (28) showed that  $\Delta$ Np73 $\alpha$  is expressed in MEFs but not in IKK $\alpha/\beta$  knockout MEFs (Fig. 1F, left panel). Also, in this case, no significant difference was observed in  $\Delta$ Np73 mRNA levels in wild-type and IKK $\alpha/\beta$  null MEFs (Fig. 1F, right panel).

Thus, an active IKK complex is correlated with the accumulation of the  $\Delta$ Np73 $\alpha$  protein without increasing its gene transcription.

**$\Delta$ Np73 $\alpha$  stabilization is dependent on IKK $\beta$  activity and does not require NF- $\kappa$ B activation.** IKK activates the transcription factor NF- $\kappa$ B by promoting degradation of I $\kappa$ B and subsequent translocation of NF- $\kappa$ B into the nucleus, where it activates the transcription of target genes (17, 18).  $\Delta$ Np73 $\alpha$  accumulation in 38E6E7HFK cells may be directly regulated by IKK complex independently of NF- $\kappa$ B activation, or it requires the transcription of specific NF- $\kappa$ B-regulated genes. To discriminate between these two possibilities, we generated a stable cell line of 38E6E7HFK that expressed a nondegradable deletion mutant of I $\kappa$ B $\alpha$  ( $\Delta$ N-I $\kappa$ B $\alpha$ ), which lacks the first 36 amino acids at the N terminus and is not regulated by IKK. Accordingly, activation of IKK by TNF- $\alpha$  in  $\Delta$ N-I $\kappa$ B $\alpha$ -expressing 38E6E7HFK cells did not result in p65 translocation to the nucleus (data not shown). In these cells, no decrease in  $\Delta$ Np73 $\alpha$  mRNA or protein levels occurred (Fig. 2A) in the presence of ectopic levels of  $\Delta$ N-I $\kappa$ B $\alpha$ . Similarly, downregulation of NF- $\kappa$ B p65 by siRNA did not alter  $\Delta$ Np73 $\alpha$  protein levels (Fig. 2B). Thus, the accumulation of  $\Delta$ Np73 $\alpha$  mediated by IKK appears to be independent of NF- $\kappa$ B. To further evaluate a direct role for IKK in  $\Delta$ Np73 $\alpha$  accumulation, we expressed IKK $\alpha$  and/or IKK $\beta$  in HEK293 cells together with  $\Delta$ Np73 $\alpha$ . IKK $\alpha$  only marginally affected  $\Delta$ Np73 $\alpha$  protein levels, while IKK $\beta$  induced strong  $\Delta$ Np73 $\alpha$  accumulation (Fig. 2C). In the same experimental model (HEK293 cells), increasing the concentration of I $\kappa$ B $\alpha$  did not affect the ability of IKK $\beta$  to stabilize  $\Delta$ Np73 $\alpha$  (Fig. 2D). Gene silencing by siRNA of IKK $\alpha$  or IKK $\beta$  in 38E6E7HFK cells confirmed that IKK $\beta$  is mainly responsible for the increased protein levels of  $\Delta$ Np73 $\alpha$  (Fig. 2E). Accordingly,  $\Delta$ Np73 $\alpha$  could be detected in IKK $\alpha$ <sup>-/-</sup> MEFs, but it is markedly lower in IKK $\beta$ <sup>-/-</sup> MEFs (Fig. 2F). Reintroduction of IKK $\beta$  into IKK $\beta$ <sup>-/-</sup> MEFs led to an increase in endogenous  $\Delta$ Np73 $\alpha$  protein levels (Fig. 2G). In addition, exposure of cells to TNF- $\alpha$ , a potent activator of IKK, led to sustained accumulation of HA- $\Delta$ Np73 $\alpha$  in IKK $\alpha$ <sup>-/-</sup> MEFs but not in IKK $\beta$ <sup>-/-</sup> cells (Fig. 2H). Finally, overexpression of IKK $\beta$  increased the stability of  $\Delta$ Np73 $\alpha$  in HEK293 cells, while inhibition of IKK $\beta$  by overexpression of DN-IKK resulted in a decrease in the half-life of endogenous  $\Delta$ Np73 $\alpha$  in 38E6E7HFK cells (Fig. 2I and J). As a whole, these data

followed by immunoblotting. "Input" represents 1/10 of total extracts used for the immunoprecipitation. As a control, immunocomplexes obtained from HEK293 cells transfected with pcDNA or pcDNA3-HA- $\Delta$ Np73 $\alpha$  were included in the experiment. (C) Primary HFK and 38E6E7HFK cells were collected and fractionated by using a nuclear extraction kit (Panomics). After fractionation, total extract (T), cytoplasm (C), and nucleus (N) were analyzed by immunoblotting with the indicated antibodies. (D) Primary HFK cells transduced with empty retrovirus (pLXSN) or 38E6E7HFK cells were seeded on coverslips. After immunofluorescent staining for  $\Delta$ Np73 and IKK $\beta$  with specific antibodies, fluorescent signal was visualized using confocal microscopy. FRET analysis was performed as explained in Materials and Methods. A representative image of a FRET positive signal for each cell line is shown in the right panels (2). As a negative control, FRET analyses were performed with cells stained only with the fluorochrome donor (Alexa 488) (1). (E) HEK293 cells were transfected with the indicated expression plasmids; 24 h posttransfection, protein extracts were immunoprecipitated and analyzed by immunoblotting. The last lane was obtained in the same experiment and was taken from a different area of the same SDS-PAGE gel. The asterisk indicates the IgG heavy chain. (F) Schematic representation of  $\Delta$ Np73 deletion mutants. (G) HEK293 cells were transfected with pcDNA3 constructs expressing wild-type or deleted HA- $\Delta$ Np73 mutants together with pcDNA3-Flag-IKK $\beta$  as indicated. After 24 h, cells were collected and protein extracts were prepared. Immunoprecipitations were performed using an anti-Flag antibody, and pellets were analyzed by immunoblotting. Input represents 1/10 of total extracts used for the immunoprecipitation. (H) HEK293 cells were transfected with pcDNA3 constructs as indicated. After 24 h, protein extracts were immunoprecipitated with an HA-tag antibody, and pellets were analyzed by immunoblotting.

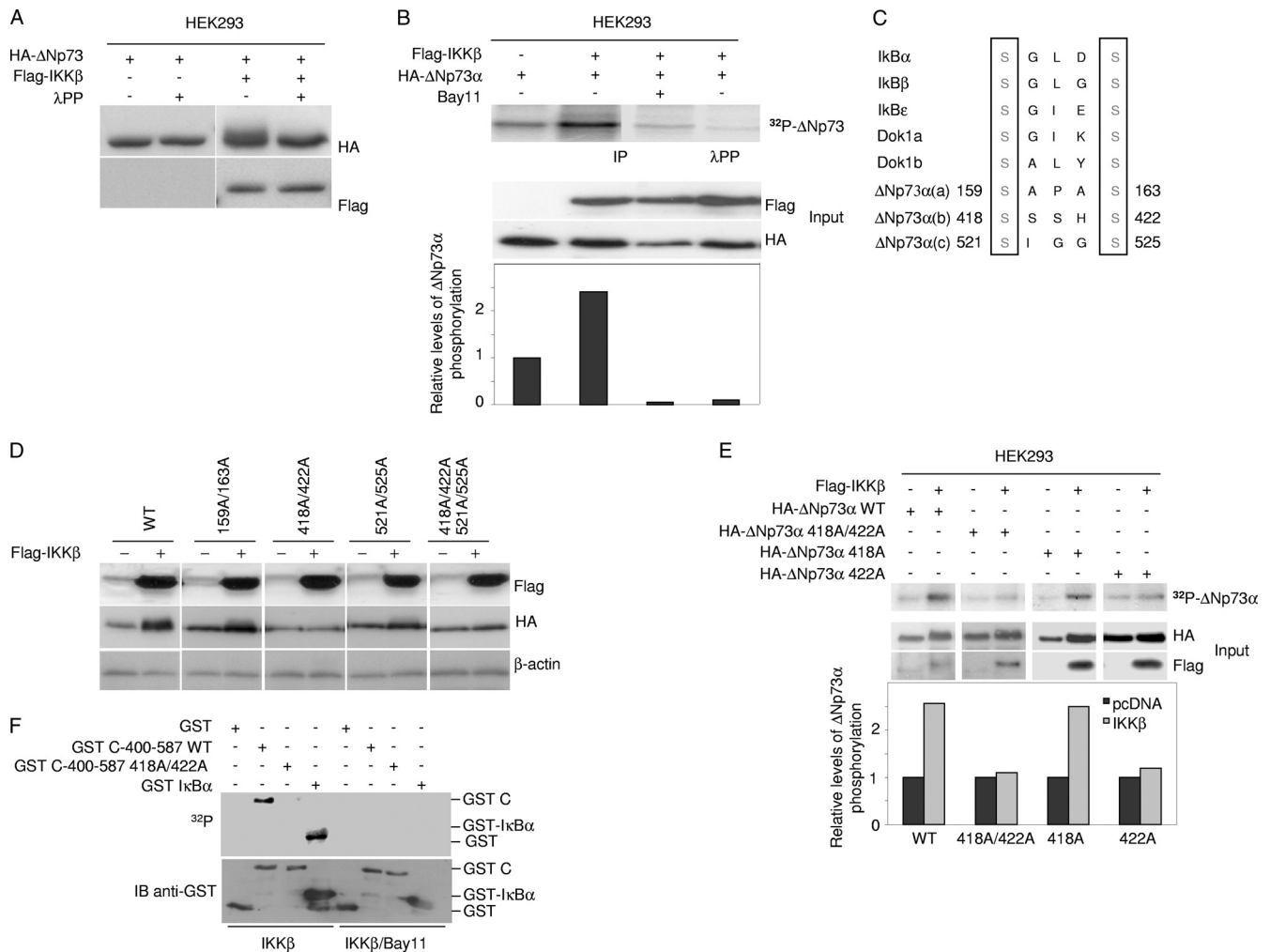


**FIG. 4.** IKK $\beta$  phosphorylates  $\Delta$ Np73. (A) HEK293 cells were transfected with expression plasmids as indicated. After 24 h, protein extracts were treated or not with  $\lambda$ PP and analyzed by immunoblotting. (B) HEK293 cells were transfected with the indicated pcDNA3 constructs and cultured in the presence of [ $^{32}$ P]orthophosphate with or without Bay11. Immunoprecipitations were performed using anti-HA-tag antibody. One immunopellet was treated with  $\lambda$ -phosphatase (top panel, fourth lane). Proteins were analyzed by autoradiography and by immunoblotting (top and lower panels, respectively). The histogram (bottom panel) shows the phosphorylation levels of the different  $\Delta$ Np73 $\alpha$  protein bands. For each band, radioactive signal was normalized to the immunoblotting signal of the input. (C) Amino acid sequence alignments of IKK phosphorylation sites of two cellular proteins that are targeted by IKK complex (I $\kappa$ B and Dok1) with potential IKK phosphorylation sites of  $\Delta$ Np73 $\alpha$ . Numbers indicate the positions of serines in  $\Delta$ Np73 $\alpha$  that are potentially phosphorylated by IKK. (D) HEK293 cells were transfected with wild-type  $\Delta$ Np73 $\alpha$  (WT) or various alanine substitution mutants with or without Flag-IKK $\beta$ . Protein extracts were analyzed by immunoblotting with the indicated antibodies. (E) HEK293 cells were transfected with the indicated constructs, and  $^{32}$ P labeling was performed as described in the legend for panel B. Immunoprecipitation was performed using anti-HA-tag antibody, followed by immunoblotting or autoradiography (top panels). The histogram (bottom panel) was obtained as explained in the legend for panel B. (F) Kinetic reactions were carried out as described in Materials and Methods using GST fusion proteins with the C-terminal domain of wild-type or 422A mutant  $\Delta$ Np73 $\alpha$  or I $\kappa$ B $\alpha$ . Radioactive and cold proteins were detected by autoradiography and immunoblotting, respectively (top and lower panels). (G) HEK293 cells were cotransfected with IKK $\beta$  and wild-type  $\Delta$ Np73 $\alpha$  or the 442A  $\Delta$ Np73 $\alpha$  mutant together with pE-GFP-PC1. Cells were seeded on coverslips and subjected to immunofluorescence analysis as described in Materials and Methods with the indicated antibodies. (H) 38E6E7HFK cells were transfected with S or AS against  $\Delta$ Np73 $\alpha$  together with the pE-GFP-PC1 construct. Thirty hours posttransfection, cells were stained with anti- $\Delta$ Np73 $\alpha$  P-422S antibody and analyzed by immunofluorescence. Representative images are shown in the left panel. Quantification of  $\Delta$ Np73 $\alpha$  P-422S and GFP-positive cells or GFP-positive cells was determined by counting at least 100 transfected cells in more than 10 different fields (right panel). (I) HFK or 38E6E7HFK cells were stained with a specific antibody against the 422S-phosphorylated form of  $\Delta$ Np73 $\alpha$ . As controls, immunofluorescence was also performed without the primary antibody (no Ab) or with primary antibody preincubated with the phosphorylated or nonphosphorylated 422S  $\Delta$ Np73 $\alpha$  peptide. (J) 38E6E7HFK cells were cotransfected with pE-GFP-PC1 and siRNAs against IKK $\alpha$  (siIKK $\alpha$ ), IKK $\beta$  (siIKK $\beta$ ), or siLuc as a negative control. Thirty hours posttransfection, cells were stained with anti- $\Delta$ Np73 $\alpha$  P-422S antibody and subjected to immunofluorescence analysis. Representative images are shown in the left panel; arrows indicate transfected cells. Quantification of  $\Delta$ Np73 $\alpha$  P-422S and GFP-positive cells or GFP-positive cells was determined by counting at least 100 transfected cells in more than 10 different fields (right panel).

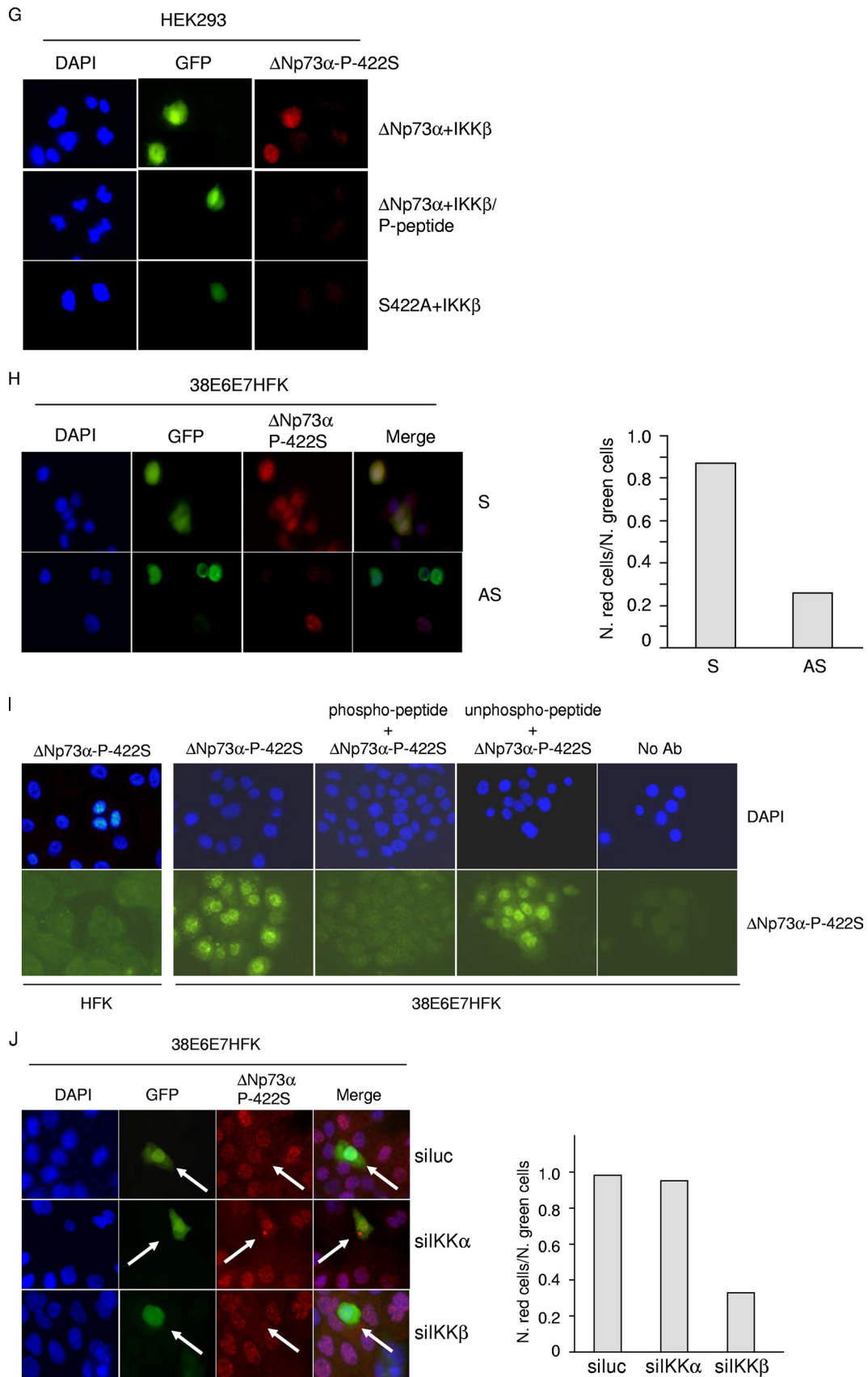


FIG. 4—Continued.

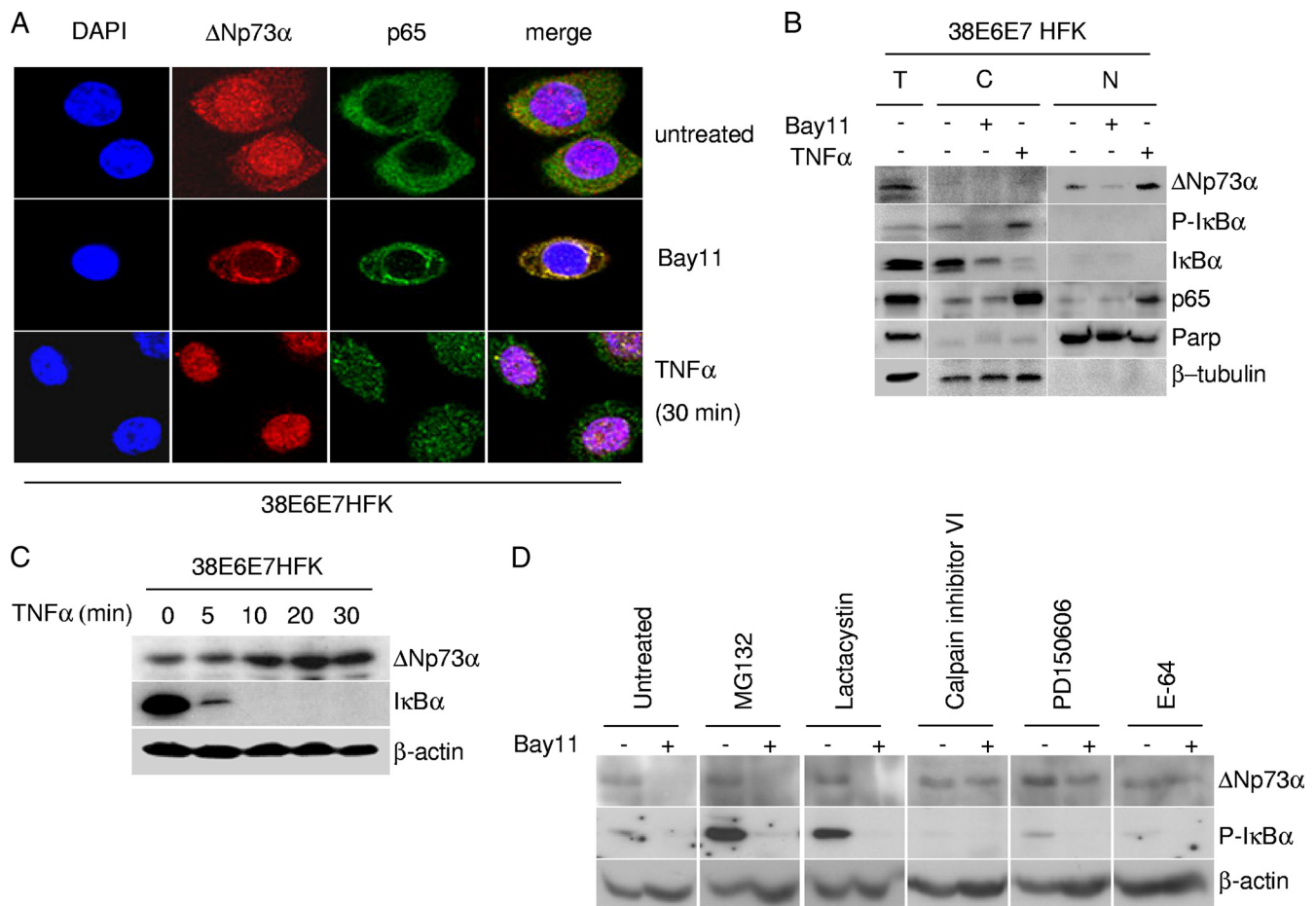


FIG. 5. IKK $\beta$  affects stability and intracellular localization of  $\Delta$ Np73 $\alpha$ . (A) 38E6E7HFK cells were treated with TNF- $\alpha$  or Bay11 and  $\Delta$ Np73 $\alpha$  and p65 cellular localization was visualized by immunofluorescence with indicated antibodies. (B) 38E6E7HFK cells treated with TNF- $\alpha$  or Bay11 were collected and fractionated by using a nuclear extraction kit (Panomics). After fractionation, total extract (T), cytoplasm (C), and nucleus (N) were analyzed by immunoblotting with the indicated antibodies. (C) 38E6E7HFK cells were treated with TNF- $\alpha$  at the indicated time points. Protein extracts were prepared and analyzed by immunoblotting using the indicated antibodies. (D) 38E6E7HFK cells were treated with the indicated protease inhibitors for 8 h and Bay11 (+) or DMSO (-) for 2 h. Protein extracts were visualized by immunoblotting. (E) HEK293 cells were transfected with the pcDNA3 HA- $\Delta$ Np73 construct and cultured under specified conditions (left and right panels) or cotransfected with different pcDNA3 constructs in the indicated combinations (right panel). Cells were then treated with indicated inhibitors followed by immunoprecipitation of whole-cell lysates and immunoblotting with the indicated antibodies. (F) 38E6E7HFK cells were seeded on coverslips and treated for 8 h with E-64 and/or for 2 h with Bay11. After the cells were fixed,  $\Delta$ Np73 was visualized by immunofluorescence with specified antibodies. (G) *In vitro*-translated HA-tagged WT and mutant 422E  $\Delta$ Np73 were incubated with recombinant calpain I in the presence or absence of Ca<sup>2+</sup>. After 30 min, the reaction was stopped by the addition of SDS loading buffer, and samples were analyzed by immunoblotting with an anti-HA-tag antibody. (H) 38E6E7HFK cells were transfected with the pcDNA3-expressing wild type or 422A or 422E HA- $\Delta$ Np73 $\alpha$ . After 24 h, protein extracts were analyzed by immunoblotting with the indicated antibodies.

provide further evidence for a direct role of IKK $\beta$  but not IKK $\alpha$  in  $\Delta$ Np73 $\alpha$  protein stability.

**IKK $\beta$  interacts with  $\Delta$ Np73 $\alpha$ .** Since we found that IKK $\beta$  influences  $\Delta$ Np73 $\alpha$  protein levels, we next evaluated whether it interacts physically with  $\Delta$ Np73 $\alpha$ . Tagged proteins, Flag-IKK $\alpha$  and/or - $\beta$  and HA- $\Delta$ Np73 $\alpha$ , were coexpressed in HEK293 cells, and immunoprecipitations were performed with a HA- or Flag-specific antibody. As shown in Fig. 3A, an IKK $\beta$ / $\Delta$ Np73 $\alpha$  complex was immunoprecipitated by the HA and Flag antibodies. A weak interaction was also observed between  $\Delta$ Np73 $\alpha$  and IKK $\alpha$  that was increased when IKK $\beta$  was also overexpressed (Fig. 3A).  $\Delta$ Np73 $\alpha$ /IKK $\alpha$  interaction may be mediated by IKK $\beta$ , which has the ability to bind both proteins, or alternatively by the IKK $\alpha$  binding site, previously characterized in

TAp73, which is also present in  $\Delta$ Np73 $\alpha$  (10). The interaction between IKK $\beta$  and  $\Delta$ Np73 $\alpha$  was also confirmed in 38E6E7HFK cells by immunoprecipitating endogenous IKK $\beta$  or  $\Delta$ Np73 $\alpha$  (Fig. 3B). We next evaluated the colocalization of the two cellular proteins by cellular fractionation and immunofluorescent staining. IKK $\beta$  was found in the cytoplasm of primary HFK cells and in the cytoplasm and nucleus in 38E6E7HFK cells by both assays (Fig. 3C). Regarding  $\Delta$ Np73 $\alpha$ , immunofluorescence staining showed that it is localized exclusively in the cytoplasm in normal keratinocytes, while it was detected in the cytoplasm and in the nucleus in 38E6E7HFK cells (Fig. 3D). In contrast,  $\Delta$ Np73 $\alpha$  appeared to be localized only in the nucleus in cellular fractionation experiments (Fig. 3C). The difference in  $\Delta$ Np73 $\alpha$  localization deter-

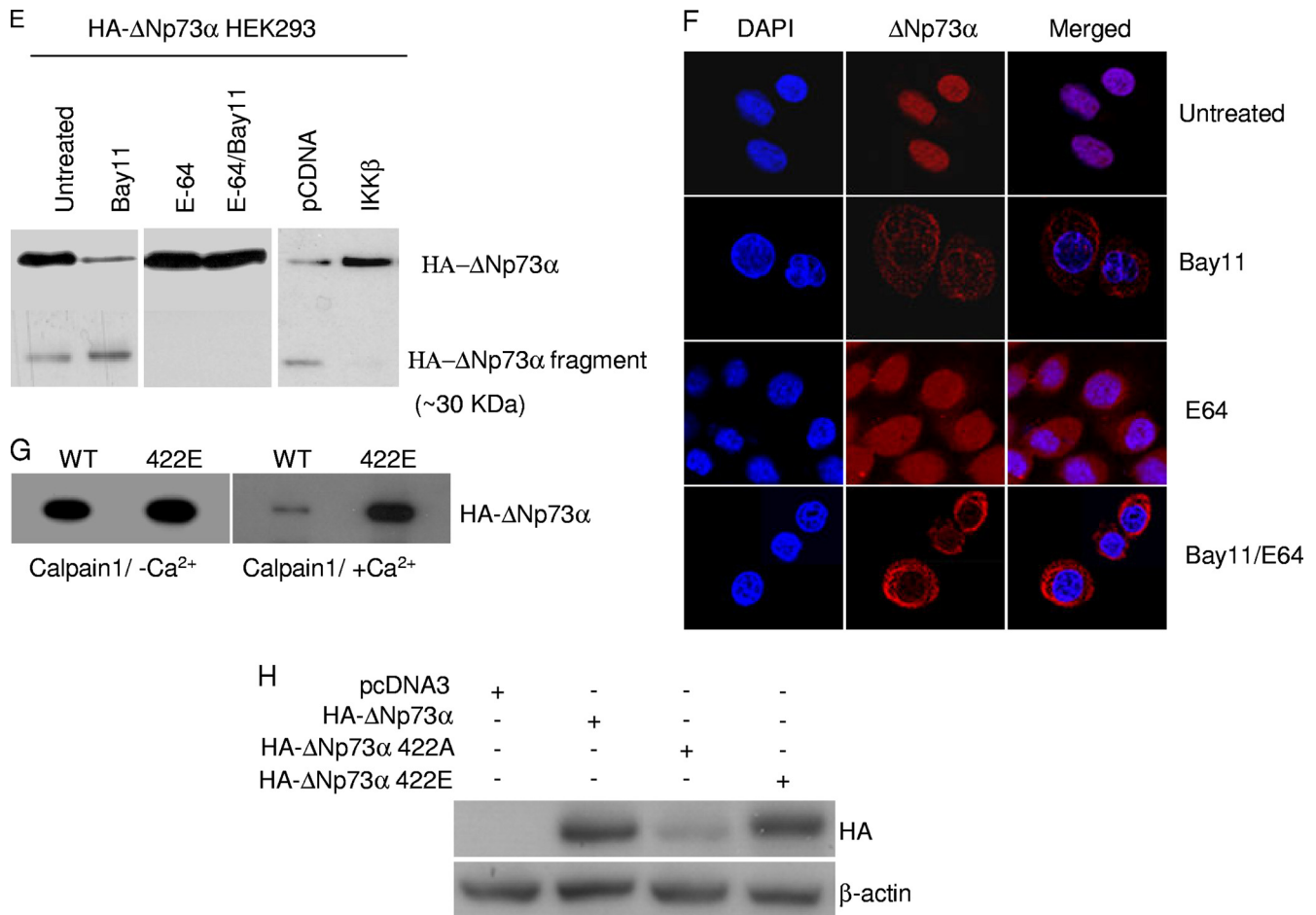


FIG. 5—Continued.

mined with the two assays may be due to the use of two different antibodies. However, FRET experiments showed that IKK $\beta$  and  $\Delta$ Np73 $\alpha$  interact in the nuclei of 38E6E7HFK cells (Fig. 3D), providing additional evidence for the interaction of the two cellular proteins. No FRET signal was detected when cells were stained only with the anti-IKK $\beta$  antibody (Fig. 3D). As an additional control, we also determined the IKK $\alpha$  cellular localization in primary or 38E6E7HFK cells, which appeared to be mainly cytoplasmic and perinuclear in both types of cells (data not shown).

To identify the region of IKK $\beta$  responsible for its interaction with  $\Delta$ Np73 $\alpha$ , two IKK $\beta$  deletion mutants, at the N and C terminuses, were expressed in HEK293 cells. The truncated IKK $\beta$  molecule containing the first 303 amino acids was able to interact with  $\Delta$ Np73 $\alpha$ , while no association was detected with the C-terminal IKK $\beta$  region (amino acids 304 to 756) (Fig. 3E). Next, we sought to identify the region of  $\Delta$ Np73 $\alpha$  involved in the interaction with IKK $\beta$ . Three  $\Delta$ Np73 $\alpha$  deletion mutants were generated and expressed in HEK293 cells (Fig. 3F). Immunoprecipitation experiments showed that only mutant C, containing the last 287 amino acids, retained the ability to bind IKK $\beta$  (Fig. 3G). Thus, IKK $\beta$  and  $\Delta$ Np73 $\alpha$  interact via their respective N and C terminuses.

Several isoforms of  $\Delta$ Np73 that differ in their C terminus

and properties have been described (23). For instance,  $\Delta$ Np73 $\beta$  is a shorter form that lacks the last 137 amino acids of  $\Delta$ Np73 $\alpha$  and exerts proapoptotic functions similarly to p53, in contrast to  $\Delta$ Np73 $\alpha$  (30). Coexpression of HA- $\Delta$ Np73 $\beta$  and Flag-IKK $\beta$  in HEK293 cells followed by immunoprecipitation with an anti-HA-tag antibody showed no interaction between the two proteins (Fig. 3H). Thus, the ability to complex with IKK $\beta$  is an exclusive property of the  $\Delta$ Np73 $\alpha$  isoform and requires the C-terminal 137 amino acids.

**IKK $\beta$  phosphorylates  $\Delta$ Np73 $\alpha$  at serine 422.** We next determined whether  $\Delta$ Np73 $\alpha$  is a substrate of IKK $\beta$ . When cotransfected with IKK $\beta$  in HEK293,  $\Delta$ Np73 $\alpha$  migrated as a diffuse band in SDS-PAGE, while treatment of the total cellular extract with  $\lambda$  serine/threonine protein phosphatase ( $\lambda$ PP) resulted in the appearance of a sharp protein band (Fig. 4A). *In vivo*  $^{32}$ P labeling experiments with HEK293 cells expressing HA- $\Delta$ Np73 $\alpha$  showed that expression of Flag-IKK $\beta$  resulted in elevated  $\Delta$ Np73 $\alpha$  phosphorylation, which was inhibited in Bay11-treated cells (Fig. 4B). In addition, incubation of the HA- $\Delta$ Np73 $\alpha$  immunopellet from IKK $\beta$ -expressing HEK293 cells with  $\lambda$ PP led to a decrease in levels of phosphorylated  $\Delta$ Np73 $\alpha$  (Fig. 4B). Collectively, these data indicate that IKK $\beta$  phosphorylates  $\Delta$ Np73 $\alpha$  at serine and/or threonine residues.

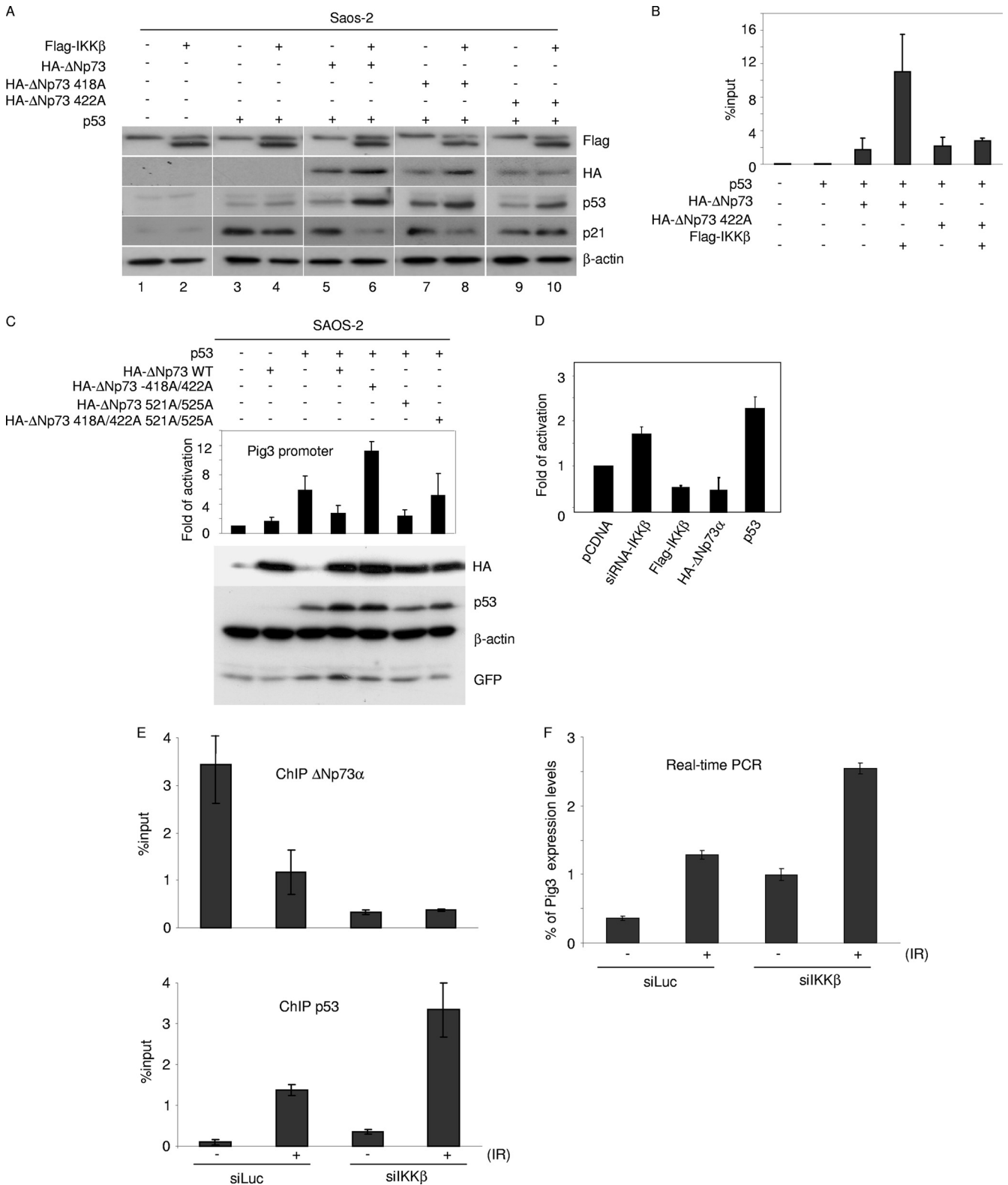


**FIG. 6.** IKK-mediated phosphorylation of  $\Delta$ Np73 $\alpha$  increases its p53 inhibitory activity. (A) Saos-2 cells were transfected with different pcDNA3 constructs in the indicated combinations. After 24 h, protein extracts were analyzed by immunoblotting with the indicated antibodies. (B) Saos-2 cells were transfected with different pcDNA3 constructs in the indicated combinations. After 36 h, ChIP was performed using an anti-HA-tag antibody and followed by real-time PCR, using primers flanking the p53 RE within the p21 promoter. Simultaneously, 1/10 of the total chromatin was processed. The values in the histogram were obtained by dividing for each sample the amount of p21 promoter which is bound by  $\Delta$ Np73-HA by the total amount of p21 promoter present in the input. (C) Saos-2 cells were transfected with the following constructs: Pig3prom-firefly luciferase

A comparison of  $\Delta$ Np73 $\alpha$  amino acid sequence with known IKK substrates (17, 20) revealed the presence of three potential IKK $\beta$  phosphorylation sites (Fig. 4C). To determine whether one or more of these sites are indeed phosphorylated by IKK $\beta$ , we generated several  $\Delta$ Np73 $\alpha$  mutants, in which the serines within the hypothetical IKK $\beta$  phosphorylation sites were mutated to alanines. The protein levels of the  $\Delta$ Np73 $\alpha$  159A 163A and 521A 525A mutants were increased in the presence of IKK $\beta$  in HEK293 cells similarly to the wild-type protein (Fig. 4D). In contrast, mutations of serines 418 and 422 decreased  $\Delta$ Np73 $\alpha$  accumulation induced by IKK $\beta$  (Fig. 4D), suggesting that phosphorylation of one or both serine residues by IKK $\beta$  plays a role in  $\Delta$ Np73 $\alpha$  accumulation. *In vivo*  $^{32}$ P labeling experiments showed that ectopic expression of IKK $\beta$  induced phosphorylation of wild-type and S418A mutant  $\Delta$ Np73 $\alpha$  in HEK293 cells, while no difference was observed with the 418A 422A and 422A mutants (Fig. 4E), indicating that S422 is the major IKK $\beta$ -induced phosphorylation site of  $\Delta$ Np73 $\alpha$ . Immunoprecipitated IKK $\beta$  also induced phosphorylation of a GST- $\Delta$ Np73 $\alpha$  C-terminus fusion protein *in vitro*, while the same fusion protein harboring the 422A mutation was not targeted by IKK $\beta$  (Fig. 4F).

In order to determine whether the phosphorylation of  $\Delta$ Np73 $\alpha$  by IKK $\beta$  at S422 occurs *in vivo* and to study the biological relevance of this modification, we next generated a rabbit polyclonal antibody against the  $\Delta$ Np73 $\alpha$  peptide that contained phosphorylated 422S. This antibody showed a weak antigen affinity in immunoblotting (data not shown), while it appeared to detect the phosphorylated form of  $\Delta$ Np73 $\alpha$  in immunofluorescence experiments. Cells expressing wild-type  $\Delta$ Np73 $\alpha$  and IKK $\beta$  showed a clear immunofluorescent signal when stained with the anti- $\Delta$ Np73 $\alpha$ -P-442S antibody, while cells expressing the  $\Delta$ Np73 $\alpha$ -422A mutant together with IKK $\beta$  were not stained (Fig. 4G). In addition,  $\Delta$ Np73 $\alpha$  downregulation decreased the staining with anti- $\Delta$ Np73 $\alpha$ -P-442S antibody, further confirming the specificity of this antibody for  $\Delta$ Np73 $\alpha$  (Fig. 4H). Immunofluorescent staining of 38E6E7HFK cells but not of primary keratinocytes revealed a strong nuclear staining that was efficiently decreased by preincubation of the antibody with the  $\Delta$ Np73 $\alpha$  phosphorylated peptide (Fig. 4I). In contrast, preincubation of the antibody with nonphosphorylated peptide only marginally affected  $\Delta$ Np73 $\alpha$  nuclear staining in 38E6E7HFK cells (Fig. 4I). Finally, downregulation of IKK $\beta$  but not IKK $\alpha$  in 38E6E7HFK cells decreased  $\Delta$ Np73 $\alpha$  staining with  $\Delta$ Np73 $\alpha$ -P-422S antibody (Fig. 4J).

Together, these data show that IKK $\beta$  phosphorylates  $\Delta$ Np73 $\alpha$  at serine 422.

**$\Delta$ Np73 $\alpha$  phosphorylation is important for nuclear accumulation and prevention of calpain-mediated degradation.** Next, we further investigated the biological significance of IKK-mediated  $\Delta$ Np73 $\alpha$  phosphorylation. Bay11 treatment of 38E6E7HFK cells resulted in a significant reduction of nuclear  $\Delta$ Np73 $\alpha$  levels (Fig. 5A). In contrast, TNF- $\alpha$ -exposed cells showed an increase in nuclear  $\Delta$ Np73 $\alpha$  levels over those of the untreated cells (Fig. 5A). Similar results were obtained with cellular fractionation experiments (Fig. 5B).  $\Delta$ Np73 $\alpha$  nuclear accumulation mediated by TNF- $\alpha$  was also evident in immunoblotting (Fig. 5C). Thus, IKK $\beta$  phosphorylation appears to favor nuclear  $\Delta$ Np73 $\alpha$  accumulation.

The decrease in  $\Delta$ Np73 $\alpha$  levels upon inhibition of IKK $\beta$  is not mediated by the proteasome pathway, since treatment with the proteasome inhibitor MG132 or lactacystin did not restore  $\Delta$ Np73 $\alpha$  levels in HPV38 E6/E7 keratinocytes cultured in the presence of Bay11, while it efficiently stabilized the phosphorylated form of I $\kappa$ B $\alpha$  that is known to be degraded by the proteasomes (Fig. 5D). However, inhibitors of the calcium-dependent proteases calpain  $\mu$  and m (calpain inhibitor VI and PD150606) were able to efficiently stabilize  $\Delta$ Np73 $\alpha$  in Bay11-treated 38E6E7HFK cells (Fig. 5D). Similar results were obtained with a general inhibitor of the cysteine proteases, E-64 (Fig. 5D). In agreement with these data, we observed that immunoblotting of cellular extracts from HA- $\Delta$ Np73 $\alpha$ -transfected HEK293 cells revealed the presence of full-length HA- $\Delta$ Np73 $\alpha$  and smaller fragments, i.e., a 30-kDa protein band (Fig. 5E, left panel). The levels of the latter protein band were increased upon Bay11 treatment (Fig. 5E, left panel), while the addition of the inhibitor of the cysteine proteases E-64 or expression of IKK $\beta$  prevented the formation of the 30-kDa HA- $\Delta$ Np73 $\alpha$  fragment (Fig. 5E, central and right panels). Simultaneous inhibition of IKK $\beta$  by Bay11 and of calpains by E-64 resulted in a cytoplasmic accumulation of  $\Delta$ Np73 $\alpha$  (Fig. 5F), indicating that the nonphosphorylated form of  $\Delta$ Np73 $\alpha$  is subject to degradation in the cytoplasm. The ability of calpain to target  $\Delta$ Np73 $\alpha$  was also observed in an *in vitro* assay. *In vitro*-translated  $\Delta$ Np73 $\alpha$  was degraded by calpain 1 but only in the presence of Ca $^{2+}$  (Fig. 5G). In contrast, the 422E  $\Delta$ Np73 $\alpha$  mutant mimicking the phosphorylated form of  $\Delta$ Np73 $\alpha$  at S422 was not efficiently targeted by calpain in the same assay (Fig. 5G), further confirming the involvement of 422S phosphorylation in  $\Delta$ Np73 $\alpha$  stability. A similar conclusion was reached by

---

reporter construct, a constitutively expressing *Renilla* construct, pcDNA3-HA- $\Delta$ Np73 $\alpha$  (wild type or 418A/422A, 521A/525A, or 418A/422A/521A/525A mutant), pcDNA-p53, and pE-GFP-IC. After 24 h, cells were collected and processed for the luciferase assay as described in Materials and Methods (upper panel). In parallel, protein extracts were prepared and analyzed by immunoblotting with the indicated antibodies (lower panel). (D) 38E6E7HFK cells were transfected with the following constructs: Pig3prom-firefly luciferase reporter construct and a constitutively expressing *Renilla* construct, in combination with siRNA-IKK $\beta$ , Flag-IKK $\beta$ , pcDNA HA- $\Delta$ Np73 $\alpha$ , or pcDNA-p53. Thirty-six hours posttransfection, cells were collected and lysed. Luciferase activity was measured and expressed as fold activation in comparison to that of the control (pcDNA). The variation in fold activities between the different conditions was significant ( $P < 0.05$ ). (E and F) 38E6E7HFK cells were transfected with siIKK $\beta$  or siLuc as a negative control; 24 h posttransfection, cells were treated with ionizing radiations (IR) (30 Gy). After irradiation, cells were allowed to grow for 8 h and processed for ChIP (E) or gene expression analysis (F). ChIP followed by real-time PCR was performed using an anti- $\Delta$ Np73 antibody (upper panel) or anti-p53 antibody (lower panel) and with primers flanking the p53-RE within the pig3 promoter. Simultaneously, 1/10 of the total chromatin was processed. The values reported in the histogram were obtained as for panel B (E). Pig3 mRNA levels in cells subjected to the indicated treatments were determined by real-time RT-PCR (F).

comparing the levels of  $\Delta$ Np73 $\alpha$  422A and 422E mutants in 38E6E7HFK cells (Fig. 5H).

Together, these data indicate that  $\Delta$ Np73 $\alpha$  is cleaved by calpain, leading to its degradation, and that this event is inhibited by IKK $\beta$ -mediated phosphorylation.

**IKK $\beta$  enhances the ability of  $\Delta$ Np73 $\alpha$  to inhibit p53 transcriptional functions.** To evaluate whether IKK $\beta$ -mediated nuclear accumulation of  $\Delta$ Np73 $\alpha$  results in downregulation of p53-regulated genes, we transfected the p53-null Saos-2 cells with p53 alone or together with IKK $\beta$  and/or  $\Delta$ Np73 $\alpha$ . As expected, p53 overexpression resulted in an increase in the endogenous protein levels of p21<sup>WAF1</sup>, by which the gene is p53-positively regulated (Fig. 6A).  $\Delta$ Np73 $\alpha$  expression reduced p53-mediated p21<sup>WAF1</sup> upregulation, a result that was further enhanced by coexpression of IKK $\beta$  (Fig. 6A). In addition, coexpression of IKK $\beta$  with the IKK $\beta$  phosphorylation mutant  $\Delta$ Np73 $\alpha$  422A did not have any effect on endogenous p21 levels, in contrast to results for the  $\Delta$ Np73 $\alpha$  418A mutant (Fig. 6A). Chromatin immunoprecipitation followed by real-time PCR revealed that IKK $\beta$  increased the binding to the p21<sup>WAF1</sup> promoter of the  $\Delta$ Np73 $\alpha$  wild type but not to that of the  $\Delta$ Np73 S422A mutant (Fig. 6B). Similar results were obtained with two additional p53-regulated promoters, i.e., Pig3 and Fas (data not shown). Transient-transfection experiments with Saos-2 cells with a construct containing the Pig3 promoter cloned in front of the luciferase reporter gene showed that only the 422A mutation affected the  $\Delta$ Np73 $\alpha$  property of counteracting p53's ability to activate the Pig3 promoter, while the other  $\Delta$ Np73 $\alpha$  mutants, the 418A, 521A, and 525A mutants, displayed an efficiency similar to that of the wild-type protein (Fig. 6C). Transient-transfection experiments with the Pig3 promoter-luciferase construct in 38E6E7HFK cells showed that silencing of IKK $\beta$  expression by siRNA induced activation of the Pig3 promoter, while ectopic expression of IKK $\beta$  resulted in an opposite effect (Fig. 6D).

Finally, to further demonstrate that IKK $\beta$  can counteract the activation of p53-regulated transcription, promoting  $\Delta$ Np73 $\alpha$  accumulation, we activated p53 in 38E6E7HFK cells by ionizing radiations (IR) in the presence or absence of IKK $\beta$ . We observed by ChIP experiments followed by real-time PCR that upon induction of DNA damage, IKK $\beta$  significantly alleviated the binding of p53 to its RE in the Pig3 promoter, due to the occupancy by  $\Delta$ Np73 $\alpha$  (Fig. 6E). In the same experiment, we determined Pig3 expression levels by real-time PCR, which correlated with the amount of p53 recruited to the Pig3 promoter in the presence or absence of IKK $\beta$  and IR (Fig. 6F).

Together, these data show that IKK $\beta$ -mediated  $\Delta$ Np73 $\alpha$  phosphorylation and accumulation result in a reduction of the transcriptional functions of p53.

**$\Delta$ Np73 $\alpha$  and IKK $\beta$  cross talk in cancer cell lines and primary cancers.** NF- $\kappa$ B is constitutively present in the nucleus of a number of human cancer cells as a result of constitutive activation of IKK (17, 18). This sustained activation of NF- $\kappa$ B contributes to the proliferation and survival of cancer cells. Therefore, we examined whether the stabilization of  $\Delta$ Np73 $\alpha$  via phosphorylation by activated IKK $\beta$  also occurs in cancer cells. We identified one head-and-neck cell line (HNC-136) and two breast cancer cell lines (HCC-1937 and Cal-51) that harbored the wild-type p53 gene and expressed  $\Delta$ Np73 $\alpha$  (Fig. 7A). Inhibition of IKK $\beta$  by Bay11 led to a decrease in  $\Delta$ Np73 $\alpha$

(Fig. 7A), indicating that IKK $\beta$  influences  $\Delta$ Np73 $\alpha$  stability in these cancer cell lines. As shown above with the other experimental models, the decreased levels of  $\Delta$ Np73 $\alpha$  upon Bay11 treatment were associated with a significant upregulation of p21<sup>WAF1</sup> (Fig. 7A). Thus, as observed in the above-described experimental models, IKK $\beta$  appears to regulate  $\Delta$ Np73 $\alpha$  in these cancer cell lines. In support of this conclusion, IKK $\beta$  and  $\Delta$ Np73 $\alpha$  were detected in the nucleus of these cell lines (Fig. 7B), while IKK $\alpha$  localized mainly in the cytoplasm (data not shown). Most importantly, FRET staining showed interaction between the two proteins (7B), which was also observed in immunoprecipitation experiments (Fig. 7C).

We next determined whether  $\Delta$ Np73 $\alpha$  is phosphorylated at serine 422 in HNC-136 and HCC-1937. Immunofluorescence stainings with  $\Delta$ Np73 $\alpha$ -P-422S antibody revealed nuclear staining in both cancer cell lines that was strongly affected by preincubation of the  $\Delta$ Np73 $\alpha$ -P-422S antibody with the phosphor peptide (Fig. 7D and F). Downregulation of  $\Delta$ Np73 $\alpha$  significantly decreased staining with the  $\Delta$ Np73 $\alpha$ -P-422S antibody, further confirming the specificity of this antibody (Fig. 7E and G).

To further evaluate the cross talk between  $\Delta$ Np73 $\alpha$  and IKK $\beta$  in cancer cells, we have analyzed normal ( $n = 2$ ) and breast cancer ( $n = 5$ ) tissues by immunohistochemistry. In four cancer tissues, we observed that IKK $\beta$  and  $\Delta$ Np73 $\alpha$  colocalized in the nucleus. In contrast, in normal tissues the two proteins were seldom detected in the nucleus (Fig. 7H). In addition, immunohistochemical stainings of normal ( $n = 2$ ) or breast cancers ( $n = 3$ ) with  $\Delta$ Np73 $\alpha$ -P-422S antibody revealed a nuclear signal only in cancer cells. Representative staining is shown in Fig. 7I.

Together, these data provide additional lines of evidence for the cross talk between IKK $\beta$  and  $\Delta$ Np73 $\alpha$ .

## DISCUSSION

Several data support the role of  $\Delta$ Np73 $\alpha$  in human carcinogenesis. Its levels have been found to be elevated in different types of human cancers, and importantly,  $\Delta$ Np73 $\alpha$ -positive cancers showed a less favorable prognosis than  $\Delta$ Np73 $\alpha$ -negative cancers (8, 22). In addition, several independent studies have demonstrated that  $\Delta$ Np73 $\alpha$  acts as a TAp73/p53 dominant-negative inhibitor, altering the cell cycle and apoptosis regulation (4, 23).

Although several mechanisms of  $\Delta$ Np73 mRNA generation have been characterized, it is still not well understood how  $\Delta$ Np73 protein stability is regulated. Here we show that  $\Delta$ Np73 $\alpha$  is a substrate of IKK $\beta$ , a key regulatory kinase of NF- $\kappa$ B activation. IKK $\beta$  phosphorylated  $\Delta$ Np73 $\alpha$  at serine 422, leading to its stabilization in the nucleus. This event is associated with the inhibition of p53/TAp73-regulated promoters, such as p21 and Pig3.

The regulation of  $\Delta$ Np73 $\alpha$  by IKK $\beta$  is unique, since the domain required for its interaction and stability is missing in the  $\Delta$ Np73 $\beta$  isoform. Interestingly, this  $\beta$  isoform, in contrast to  $\Delta$ Np73 $\alpha$ , exerts a proapoptotic function, and its levels are not affected by IKK $\beta$ . These data further highlight the role of the IKK $\beta$ / $\Delta$ Np73 $\alpha$  interaction in promoting cellular proliferation. Inhibition of IKK $\beta$  by different means induced rapid degradation of  $\Delta$ Np73 $\alpha$  via a calpain-mediated mechanism. A

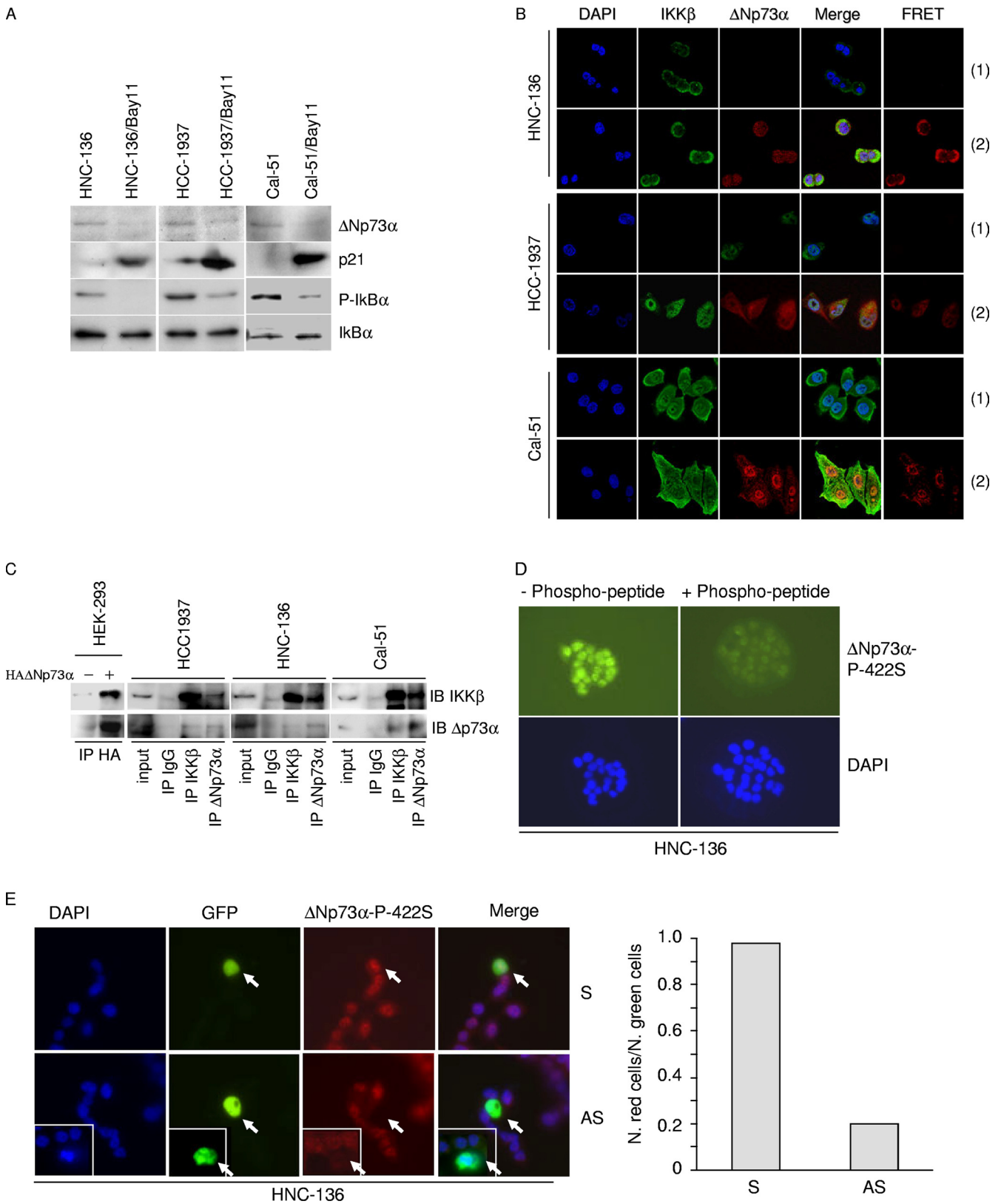
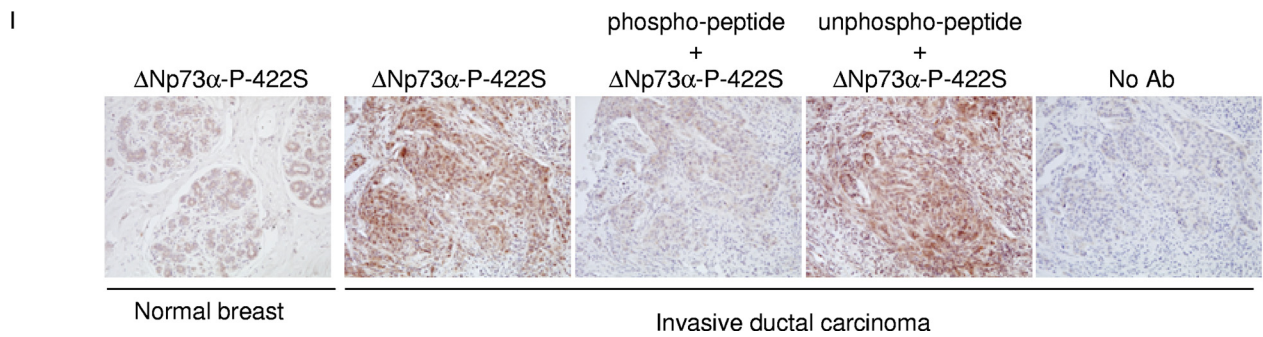
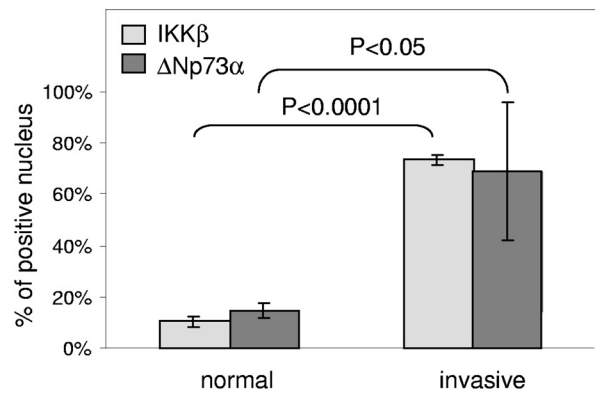
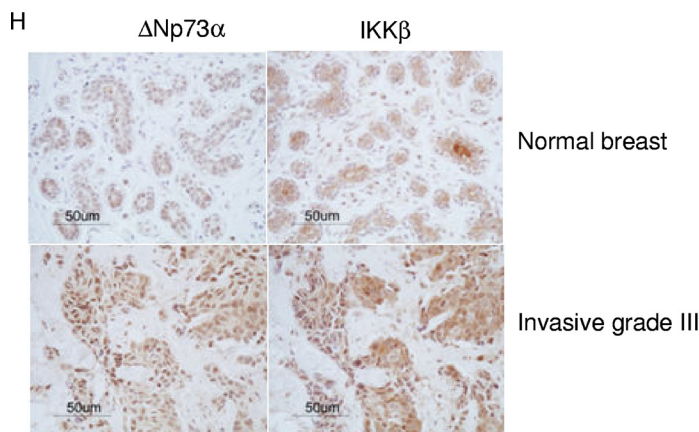
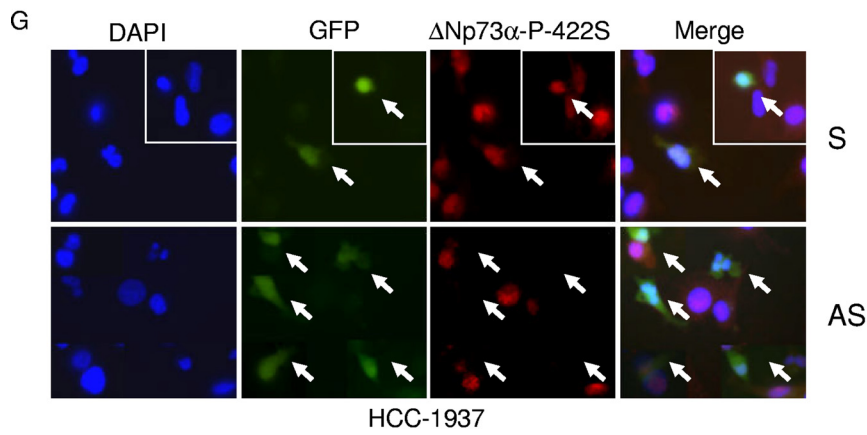
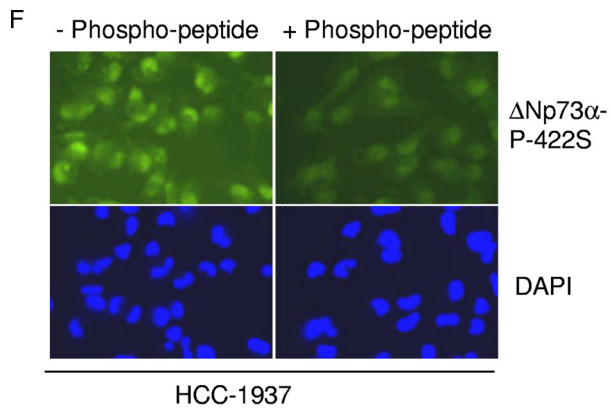


FIG. 7—Continued on following page



previous study has reported that several p73 forms, including  $\Delta$ Np73 $\alpha$ , are targeted by calpain (25). Our findings demonstrate that  $\Delta$ Np73 $\alpha$  stability is regulated by posttranslational modification. In fact, simultaneous inhibition of IKK $\beta$  and calpain resulted in  $\Delta$ Np73 $\alpha$  accumulation in the cytoplasm, suggesting that the hypophosphorylated form of  $\Delta$ Np73 $\alpha$  is processed in this cellular compartment. However, our data do not exclude that in addition to calpain, other cellular pathways may be involved in the regulation of protein levels of the unphosphorylated form of  $\Delta$ Np73 $\alpha$ .

Although our data demonstrate a link between IKK $\beta$ -induced phosphorylation and nuclear accumulation of  $\Delta$ Np73 $\alpha$ , its precise mechanisms of translocation into the nucleus remain to be elucidated. Two possible scenarios can be envisaged. IKK $\beta$  could interact and phosphorylate  $\Delta$ Np73 $\alpha$  in the cytoplasm and be transported together into the nucleus. Alternatively, IKK $\beta$  is transported into the nucleus by an independent mechanism, where it phosphorylates  $\Delta$ Np73 $\alpha$ . While the unphosphorylated  $\Delta$ Np73 $\alpha$  could freely shuttle between the nucleus and cytoplasm, it is possible that after phosphorylation it is retained in the nuclear compartment. Studies are in progress to address these issues. The observation that viral oncoproteins such as E6 and/or E7 from HPV38 can trigger IKK $\beta$  nuclear localization may facilitate our understanding of the mechanisms controlling IKK $\beta$  subcellular localization.

The ability to influence  $\Delta$ Np73 $\alpha$  levels appears to be a specific property of IKK $\beta$ , since IKK $\alpha$  interacted weakly with  $\Delta$ Np73 $\alpha$ , and inhibition of IKK $\alpha$  expression in human and rodent cells did not affect  $\Delta$ Np73 $\alpha$  stability. Interestingly, a recent study has described that IKK $\alpha$  but not IKK $\beta$  regulates stability, nuclear accumulation, and functions of TAp73 (10). Similarly to what we have observed for IKK $\beta$  and  $\Delta$ Np73 $\alpha$ , these events correlate with translocation of IKK $\alpha$  into the nucleus. A model can be proposed in which the activation of the mechanisms responsible for IKK $\alpha$  or IKK $\beta$  nuclear accumulation favor apoptosis or proliferation via stabilization of TAp73 or  $\Delta$ Np73 $\alpha$ , respectively. Interestingly, an additional study has recently shown that IKK $\beta$  phosphorylates p53 at two specific serines, promoting its ubiquitination and degradation

by  $\beta$ -TrCP1 and independently of MDM2 and NF- $\kappa$ B (31). Taking into consideration our data and those of Xia's study (31), IKK $\beta$  appears to modulate p53 transcriptional activity through two independent mechanisms, the first promoting its phosphorylation and destabilization and the second inducing phosphorylation and accumulation of the p53 antagonist  $\Delta$ Np73 $\alpha$ . This model underlines the key role of IKK $\beta$  in carcinogenesis, which indeed could be a potential target for novel anticancer therapeutic strategies. Several independent studies have identified novel nuclear functions of IKK $\alpha$  and IKK $\beta$  in the regulation of cellular gene expression and proliferation (3, 9, 32), further supporting the key role of these kinases in the nucleus independently of their ability to promote NF- $\kappa$ B nuclear translocation. During carcinogenesis, mechanisms that regulate the nuclear localization of IKK $\alpha$  or IKK $\beta$  may be altered, with consequent accumulation of  $\Delta$ Np73 $\alpha$  and loss of TAp73 functions. Our initial screening of cancer-derived cell lines and primary cancers indicates that IKK $\beta$  can be found in the nuclei of cancer cells. In addition, the IKK $\beta$  nuclear localization showed a tight correlation with  $\Delta$ Np73 $\alpha$  accumulation. Interestingly, inhibition of IKK activity in these cancer cell lines corresponded with a rescue of p53 transcriptional functions and an increase in their sensitivity to chemotherapeutic drugs (R. Accardi, unpublished data), consistent with the downregulation of the  $\Delta$ Np73 $\alpha$  levels.

We have previously shown that the E6 and E7 oncoproteins from cutaneous HPV38 activate  $\Delta$ Np73 $\alpha$  transcription (1). In this study, we show that in addition to upregulation of the  $\Delta$ Np73 $\alpha$  mRNA levels, HPV38 E6 and E7 are able to increase  $\Delta$ Np73 $\alpha$  stability. Our preliminary data on Epstein-Barr virus show that its major oncoprotein LMP1, a strong activator of IKK and the NF- $\kappa$ B pathway (29), promotes  $\Delta$ Np73 $\alpha$  accumulation (Accardi, unpublished), suggesting that this mechanism is shared with other viruses.

In summary, our data describe a novel mechanism linking two cellular proteins, IKK $\beta$  and  $\Delta$ Np73 $\alpha$ , that play a key role in human carcinogenesis.

FIG. 7. IKK $\beta$  and  $\Delta$ Np73 $\alpha$  cross talk in cancer-derived cell lines and primary cancers. (A) HNC-136, HCC-1937, and Cal-51 cell lines were treated with Bay11 for 2 h, and total protein extracts were analyzed by immunoblotting with the indicated antibodies. (B) HCC-1937, HNC-136, and Cal-51 cells were stained with the indicated antibodies. Fluorescent staining was visualized by confocal microscopy. FRET positive signals (2) and FRET negative controls (1) are shown in the right panels. (C) One-milligram protein extracts of HCC-1937, HNC-136, and Cal-51 were immunoprecipitated with an anti-IKK $\beta$  or - $\Delta$ Np73 $\alpha$  antibody. As negative controls, the same amounts of total extracts from each cell line were immunoprecipitated with anti-IgG. Immunocomplexes were analyzed by immunoblotting. One-tenth of total extracts used for the immunoprecipitation was loaded as input. As a control, immunocomplexes obtained from HEK293 cells transfected with pcDNA or pcDNA3-HA- $\Delta$ Np73 $\alpha$  were included in the experiment. (D) HNC-136 cells were stained with the indicated antibodies. Fluorescent staining was visualized by confocal microscopy. As a control, primary antibody was preincubated with an excess of 422S-phosphorylated peptide. (E) HNC-136 cells were cotransfected with pE-GFP-IC and S or AS against  $\Delta$ Np73 $\alpha$ . Thirty hours posttransfection, cells were stained with anti- $\Delta$ Np73 $\alpha$  P-422S antibody and analyzed for immunofluorescence. Representative images are shown in the left panel; arrows indicate transfected cells. The white frame indicates a different field. Quantification of  $\Delta$ Np73 $\alpha$  P-422S and GFP-positive cells or GFP-positive cells was determined by counting at least 100 transfected cells in more than 10 different fields (right panel). (F) HCC-1937 cells were stained as explained in the legend for panel D. (G) HCC-1937 cells were transfected and processed as explained in the legend for panel E. Representative images are shown in the left panel; arrows indicate transfected cells. The white frame indicates a different field. Quantification of  $\Delta$ Np73 $\alpha$  P-422S and GFP-positive cells or GFP-positive cells was determined by counting at least 100 transfected cells in more than 10 different fields (right panel). (H)  $\Delta$ Np73 and IKK $\beta$  cellular localization was analyzed in normal and cancer breast tissues (left panel, representative staining). The histogram (right panel) shows the quantification of the percentage of cells in normal ( $n = 1$ ) or cancer tissues ( $n = 3$ ) with nuclear staining for IKK $\beta$  and  $\Delta$ Np73 $\alpha$ . (I) Normal and breast cancer tissues were stained with a specific antibody against the 422S-phosphorylated form of  $\Delta$ Np73 $\alpha$ . As controls, immunostaining was also performed without the primary antibody (no Ab) or with primary antibody preincubated with a phosphorylated or nonphosphorylated 422S  $\Delta$ Np73 $\alpha$  peptide.

## ACKNOWLEDGMENTS

We are grateful to all members of the Infections and Cancer Biology group for their support, to Lucien Frappart, Thomas Gilmore, David Goeddel, Elliot Kieff, Alain Puisieux, and Inder Verma for kindly providing reagents and/or specimens, to the Common Centre of Quantimetry CCQ (UBCL, Lyon, France) for immunohistological analyses, and to John Daniel and Uzma Hasan for critical reading of the manuscript.

This study was supported partially by grants to B.S.S. from La Ligue Contre le Cancer (Comité du Rhône and Drôme) and by grants to M.T. from La Ligue Contre le Cancer (Comités du Rhône, Drôme and Savoie), Association pour la Recherche sur le Cancer, European Union (LSHC-2005-018704), and Association for International Cancer Research, as well as grants to M.T. and L.G. from DKFZ-Cancéropôle Grand-Est, German-French cooperation program.

## REFERENCES

1. **Accardi, R., et al.** 2006. Skin human papillomavirus type 38 alters p53 functions by accumulation of deltaNp73. *EMBO Rep.* **7**:334–340.
2. **Agami, R., G. Blandino, M. Oren, and Y. Shaul.** 1999. Interaction of c-Abl and p73alpha and their collaboration to induce apoptosis. *Nature* **399**:809–813.
3. **Anest, V., et al.** 2003. A nucleosomal function for IkappaB kinase-alpha in NF-kappaB-dependent gene expression. *Nature* **423**:659–663.
4. **Buhlmann, S., and B. M. Putzer.** 2008. DNp73 a matter of cancer: mechanisms and clinical implications. *Biochim. Biophys. Acta* **1785**:207–216.
5. **Caldeira, S., et al.** 2003. The E6 and E7 proteins of cutaneous human papillomavirus type 38 display transforming properties. *J. Virol.* **77**:2195–2206.
6. **Clegg, R. M.** 1992. Fluorescence resonance energy transfer and nucleic acids. *Methods Enzymol.* **211**:353–388.
7. **Costanzo, A., et al.** 2002. DNA damage-dependent acetylation of p73 dictates the selective activation of apoptotic target genes. *Mol. Cell* **9**:175–186.
8. **Dominguez, G., et al.** 2006. DeltaTAp73 upregulation correlates with poor prognosis in human tumors: putative in vivo network involving p73 isoforms, p53, and E2F-1. *J. Clin. Oncol.* **24**:805–815.
9. **Fu, L., et al.** 2009. BAFF-R promotes cell proliferation and survival through interaction with IKKbeta and NF-kappaB/c-Rel in the nucleus of normal and neoplastic B-lymphoid cells. *Blood* **113**:4627–4636.
10. **Furuya, K., et al.** 2007. Stabilization of p73 by nuclear IkappaB kinase-alpha mediates cisplatin-induced apoptosis. *J. Biol. Chem.* **282**:18365–18378.
11. **Gong, J. G., et al.** 1999. The tyrosine kinase c-Abl regulates p73 in apoptotic response to cisplatin-induced DNA damage. *Nature* **399**:806–809.
12. **Gonzalez, S., C. Prives, and C. Cordon-Cardo.** 2003. p73alpha regulation by Chk1 in response to DNA damage. *Mol. Cell. Biol.* **23**:8161–8171.
13. **Grob, T. J., et al.** 2001. Human delta Np73 regulates a dominant negative feedback loop for TAp73 and p53. *Cell Death Differ.* **8**:1213–1223.
14. **Haupt, Y., R. Maya, A. Kazaz, and M. Oren.** 1997. Mdm2 promotes the rapid degradation of p53. *Nature* **387**:296–299.
15. **Ishimoto, O., et al.** 2002. Possible oncogenic potential of DeltaNp73: a newly identified isoform of human p73. *Cancer Res.* **62**:636–641.
16. **Jost, C. A., M. C. Marin, and W. G. Kaelin, Jr.** 1997. p73 is a simian [correction of human] p53-related protein that can induce apoptosis. *Nature* **389**:191–194. (Erratum, **399**:817, 1999.)
17. **Karin, M.** 2006. Nuclear factor-kappaB in cancer development and progression. *Nature* **441**:431–436.
18. **Karin, M.** 2008. The IkappaB kinase—a bridge between inflammation and cancer. *Cell Res.* **18**:334–342.
19. **Lee, C. W., and N. B. La Thangue.** 1999. Promoter specificity and stability control of the p53-related protein p73. *Oncogene* **18**:4171–4181.
20. **Lee, S., et al.** 2004. IkappaB kinase beta phosphorylates Dok1 serines in response to TNF, IL-1, or gamma radiation. *Proc. Natl. Acad. Sci. U. S. A.* **101**:17416–17421.
21. **Liu, G., S. Nozell, H. Xiao, and X. Chen.** 2004. DeltaNp73beta is active in transactivation and growth suppression. *Mol. Cell. Biol.* **24**:487–501.
22. **Lunghi, P., et al.** 2006. MEK1 inhibition sensitizes primary acute myelogenous leukemia to arsenic trioxide-induced apoptosis. *Blood* **107**:4549–4553.
23. **Melino, G., V. De Laurenzi, and K. H. Vousden.** 2002. p73: friend or foe in tumorigenesis. *Nat. Rev. Cancer* **2**:605–615.
24. **Morgenstern, J. P., and H. Land.** 1990. Advanced mammalian gene transfer: high titre retroviral vectors with multiple drug selection markers and a complementary helper-free packaging cell line. *Nucleic Acids Res.* **18**:3587–3596.
25. **Munarriz, E., et al.** 2005. Calpain cleavage regulates the protein stability of p73. *Biochem. Biophys. Res. Commun.* **333**:954–960.
26. **Nieminen, J., A. Kuno, J. Hirabayashi, and S. Sato.** 2007. Visualization of galectin-3 oligomerization on the surface of neutrophils and endothelial cells using fluorescence resonance energy transfer. *J. Biol. Chem.* **282**:1374–1383.
27. **Ren, J., et al.** 2002. p73beta is regulated by protein kinase Cdelta catalytic fragment generated in the apoptotic response to DNA damage. *J. Biol. Chem.* **277**:33758–33765.
28. **Rossi, M., et al.** 2005. The ubiquitin-protein ligase Itch regulates p73 stability. *EMBO J.* **24**:836–848.
29. **Sylla, B. S., et al.** 1998. Epstein-Barr virus-transforming protein latent infection membrane protein 1 activates transcription factor NF-kappaB through a pathway that includes the NF-kappaB-inducing kinase and the IkappaB kinases IKKalpha and IKKbeta. *Proc. Natl. Acad. Sci. U. S. A.* **95**:10106–10111.
30. **Ueda, Y., M. Hijikata, S. Takagi, T. Chiba, and K. Shimotohno.** 1999. New p73 variants with altered C-terminal structures have varied transcriptional activities. *Oncogene* **18**:4993–4998.
31. **Xia, Y., et al.** 2009. Phosphorylation of p53 by IkappaB kinase 2 promotes its degradation by beta-TrCP. *Proc. Natl. Acad. Sci. U. S. A.* **106**:2629–2634.
32. **Yamamoto, M., et al.** 1994. Effect of tumor suppressors on cell cycle-regulatory genes—Rb suppresses P34(Cdc2) expression and normal p53 suppresses cyclin A expression. *Exp. Cell Res.* **210**:94–101.
33. **Yuan, Z. M., et al.** 1999. p73 is regulated by tyrosine kinase c-Abl in the apoptotic response to DNA damage. *Nature* **399**:814–817.
34. **Zaika, A. I., et al.** 2002. DeltaNp73, a dominant-negative inhibitor of wild-type p53 and TAp73, is up-regulated in human tumors. *J. Exp. Med.* **196**:765–780.